

ELIAS FEITOSA ARAUJO

**THE INFLUENCE OF THE TARGET OF RAPAMYCIN (TOR) ON STARCH  
METABOLISM IN *Arabidopsis thaliana***

Dissertation presented to the Federal  
University of Viçosa as part of the  
requirements of the Plant Physiology  
Graduate Program to obtain the title of  
*Magister Scientiae*.

VIÇOSA  
MINAS GERAIS – BRAZIL  
2016

**Ficha catalográfica preparada pela Biblioteca Central da Universidade  
Federal de Viçosa - Câmpus Viçosa**

T

A663i  
2016

Araujo, Elias Feitosa, 19-

The influence of the Target of Rapamycin (TOR) on starch metabolism in *Arabidopsis thaliana* / Elias Feitosa Araujo. – Campinas, SP, 2016.

vii, 51f. : il. (algumas color.) ; 29 cm.

Orientador: Camila Caldana.

Dissertação (mestrado) - Universidade Federal de Viçosa.

Referências bibliográficas: f.43-50.

1. *Arabidopsis thaliana*. 2. Planta - Crescimento. 3. Planta - Metabolismo. 4. Quinases. 5. Amido. I. Universidade Federal de Viçosa. Departamento de Biologia Vegetal. Programa de Pós-graduação em Fisiologia Vegetal. II. Título.

CDD 22. ed. 583.64

ELIAS FEITOSA ARAUJO

**THE INFLUENCE OF THE TARGET OF RAPAMYCIN (TOR) ON STARCH  
METABOLISM IN *Arabidopsis thaliana***

Dissertation presented to the Federal  
University of Viçosa as part of the  
requirements of the Plant Physiology  
Graduate Program to obtain the title of  
*Magister Scientiae*.

APPROVED: February 22, 2016

---

Carlos Takeshi Hotta

---

Michel Georges Albert Vincentz

---

Camila Caldana  
(Advisor)

## **Acknowledgements**

I would like to thank my father and my mother for all the love, support and admiration. Thank you to my sisters for all the support and true friendship. I also thank my beloved niece who makes my days happier simply by listening to her voice and for her affection. Love you!

I am very grateful to my supervisor Dr. Camila Caldana for all her teaching, for allowing me to work in her laboratory, for all corrections, good humor and especially the confidence in my work. I have great admiration for her intelligence.

Many thanks to the group of Molecular Plant Physiology at CTBE for all the help during this time, shared teachings and the good moments of conviviality. Thanks to Marina for all protocols and corrections, Vivi for your friendship and patience in teaching me to do Western and taking me several times in distant laboratories to perform analyses, Flavinha for her shy smile and laugh every morning.

Thank you Japinha, person more than special, who made my year extremely happy due to her good humor and friendship. I want to especially thank two lovely friends I made during this year, Carolzinha and Val: I have enormous affection for you! Thank you very much for the good moments, laugh, and teachings. I will always remember the precious time I spent with you. Love you!

Thank you to my big friend Carla for the true friendship and for the helpings when I needed. I know I can count on her whenever I need. To my dear friends, Márcio, Vônei and Cadu for the lovely and important friendship in our house. Many thanks also to Gilmar, Tiago, Paulinho, Tom and Pedro for the very happy moments spent together. To my family and all friends that are distant but I can feel close to me. I love you!

I am also grateful to FAPEMIG (process number - 30594/14) for financial support.

## Table of contents

<b>Abstract</b> .....	iv
<b>Resumo</b> .....	vi
<b>1 - Introduction</b> .....	1
1.1 - Target of Rapamycin (TOR) signaling pathway .....	1
1.2 - Carbon metabolism in plants .....	6
1.3 - Biosynthesis of starch .....	7
1.4 - Starch degradation .....	9
1.5 - Regulation of starch metabolism .....	10
1.6 - Evidences for the influence of TOR on starch metabolism .....	15
<b>2 - Objectives</b> .....	18
<b>3 - Material and Methods</b> .....	19
3.1 - Chemicals.....	19
3.2 - Plant material and growth conditions.....	19
3.3 - Hydroponic system for <i>Arabidopsis</i> seedlings.....	19
3.4 - Inhibition of the Target of Rapamycin (TOR) by AZD-8055.....	19
3.5 - Qualitative determination of starch content by lugol iodine.....	20
3.6 - Quantification of starch by enzymatic assay.....	20
3.7 - Quantification of primary metabolites .....	21
3.8 – Gene expression analysis .....	22
3.9 - Maximal catalytic activity of ADP-glucose pyrophosphorylase (AGPase).....	22
3.10 - Immunoblotting analysis of ADP-glucose pyrophosphorylase (AGPase).....	23
3.11 - Measurement of reduced and oxidized glutathione .....	23
<b>4 - Results and Discussion</b> .....	25
4.1 - Establishment of a hydroponic growth system to investigate the role of TOR on <i>Arabidopsis</i> seedlings.....	25
4.2 - TOR–inhibited plants have increased starch synthesis .....	29
4.3 - Repression of TOR complex impacts metabolites related to starch metabolism .....	32
4.4 – Analyses of gene expression, catalytic activity and immunoblotting of ADP-glucose pyrophosphorylase (AGPase).....	35
4.5 – Measurement of reduced and oxidized glutathione and the cellular redox status .....	38
<b>5 - Conclusions</b> .....	41
<b>References</b> .....	43
<b>Supplemental data</b> .....	51

## **Abstract**

ARAUJO, Elias Feitosa, M. Sc., Universidade Federal de Viçosa. February, 2016. **The influence of the Target of Rapamycin (TOR) on starch metabolism in *Arabidopsis thaliana*.** Advisor: Camila Caldana.

Plant growth and development are maintained by a complex network controlled by environmental factors including the availability of water, light and nutrients and by several signaling pathways. One of the most important signaling pathways, conserved in eukaryotes, is the kinase Target of Rapamycin (TOR). Various lines of evidence point out that TOR plays a fundamental role in carbon and nitrogen balance, acting as an essential regulator on central metabolism by controlling growth and biomass production. Starch is the major form of carbon storage and its content is negatively correlated with growth. Transgenic lines with reduced expression of TOR gene or components of the TOR complex present a clear starch excess phenotype. However, it remained to be elucidated whether the accumulation of starch is due to increased synthesis, impaired degradation or both. In this work, *Arabidopsis* seedlings treated with the specific ATP-competitive inhibitor of TOR kinase AZD-8055 showed a starch excess phenotype right after 4 hours of treatment and the accumulation of starch was proved to be due to an augmentation in the rate of starch synthesis. Furthermore, TOR-inhibited plants presented an average increase of 20-30% in their starch content at the end of day when compared to control. Metabolite profiling analysis showed that TOR-inhibited plants exhibited broad changes in the levels of sucrose, fructose, glucose, maltose, mannose and orthophosphate, which are associated directly or indirectly with starch metabolism. In addition, a correlation between the amount of mannose, orthophosphate and increased starch content was noticed in AZD-treated plants. Gene expression analysis of AGPase subunits showed significant changes only from 18 and 24h after treatment. Although TOR inhibited plants displayed higher content of the active form of AGPase (monomer), enzymatic activity assays revealed that changes in AGPase activity might occur as secondary effect of TOR inhibition and might be not related to the starch excess phenotype observed 4 hours after AZD-treatment. Since several enzymes related to starch metabolism are subject to redox regulation, the levels of glutathione were measured to verify the redox environment of the cells. TOR-inhibited plants showed changes in the pools of glutathione, mainly in its reduced form, and the redox state of the cells tended to be more reduced. Together, these results

indicate the participation of TOR signalling on starch metabolism but the mechanistic behind this process need further studies.

## Resumo

ARAUJO, Elias Feitosa, M. Sc., Universidade Federal de Viçosa. Fevereiro de 2016. **A influência da via Target of Rapamycin (TOR) no metabolismo de amido em *Arabidopsis thaliana***. Orientadora: Camila Caldana.

O crescimento e o desenvolvimento vegetal são controlados por uma complexa rede metabólica controlada por fatores ambientais, incluindo a disponibilidade de água, nutrientes e luz, e por várias vias de sinalização. Uma das mais importantes vias de sinalização, conservada em eucariotos, é a kinase Target of Rapamycin (TOR). Várias linhas de evidência demonstram que TOR exerce um papel fundamental no balanço de carbono e nitrogênio, agindo como um regulador essencial do metabolismo central, controlando o crescimento e a produção de biomassa. O amido é a principal forma de armazenamento de carbono e seu conteúdo é correlacionado negativamente com crescimento. Linhas transgênicas com expressão reduzida do gene TOR ou dos componentes do complexo apresentam um claro fenótipo de acúmulo de amido. No entanto, ainda não é elucidado se o acúmulo de amido é devido a um aumento na síntese, decréscimo na degradação ou ambos. Neste trabalho, plântulas de *Arabidopsis* tratadas com o inibidor químico específico de TOR AZD-8055, que age no sítio de ligação do ATP no domínio quinase de TOR, mostraram um fenótipo de acúmulo de amido logo após 4 horas de tratamento e este acúmulo é devido a um aumento nas taxas de síntese deste polímero. Além disso, plântulas onde TOR estava inibida apresentaram um aumento em torno de 30-40% em seu conteúdo de amido em comparação ao controle. Análise de perfil metabólico em plântulas com inibição de TOR apresentaram mudanças nos níveis de sacarose, frutose, glicose, maltose, manose e fosfato inorgânico. Todos estes metabólitos estão correlacionados direta ou indiretamente com o metabolismo de amido. Uma correlação entre o teor de manose, fosfato inorgânico e aumento de amido foi notável em plantas tratadas com AZD-8055. Análise de expressão gênica de subunidades da AGPase apresentou mudanças significativas nos pontos 18 e 24 horas após o tratamento com o inibidor. Atividade catalítica máxima da AGPase foi determinada nos pontos 2, 4, 6, 10 e 24 horas após a administração de AZD-8055. No entanto, a atividade só foi estatisticamente diferente entre tratamentos nos pontos 4 e 24 horas. Immunoblotting para esta enzima mostrou que após 4 horas de inibição da via TOR, o conteúdo de AGPase em sua forma dimérica tendeu a ser maior em plantas controle. Além disso, o teor total de AGPase e seu conteúdo na forma monomérica foram maiores em plantas tratadas com AZD-8055 após 6 horas de tratamento na luz.



Sabendo que várias enzimas relacionadas ao metabolismo do amido são reguladas pelo potencial redox da célula, os níveis de glutathione foram mensurados para verificar o potencial redox celular. Plantas tratadas com AZD-8055 apresentaram mudanças na quantidade total de glutathione, principalmente na sua forma reduzida e o potencial redox da célula tendeu a ficar mais reduzido. Em conjunto, estes resultados indicam a participação de TOR no metabolismo do amido, mas o exato mecanismo por trás disso ainda está longe de ser elucidado.

## 1 - Introduction

### 1.1 - Target of Rapamycin (TOR) signaling pathway

As sessile organisms, plants are subject to different environmental conditions, such as availability of nutrients and water, protection from high light radiation, heavy rains, pest and pathogen attacks. Therefore, to sustain growth, plants must balance their energetic status in harmony with anticipated and stressful changes in the environment (Smith and Stitt, 2007; Xiong and Sheen, 2014). Recent studies have mapped out the signaling pathways controlling this complex network (Robaglia *et al.*, 2012). One of the most characterized growth regulator and conserved in all eukaryotes is the kinase Target of Rapamycin (TOR). This protein integrates external and internal factors and controls a wide range of anabolic and catabolic processes including transcription, translation, carbon metabolism and autophagy; promoting growth, survival and longevity (Caldana *et al.*, 2013).

TOR is a large protein of approximately 280 kD belonging to the family of protein kinases “phosphatidylinositol 3-like protein kinases” (PIKKs). TOR was found in the yeast *Saccharomyces cerevisiae* in a screen for mutants resistant to the cytostatic effects of the anti-mycotic rapamycin (Tsang *et al.*, 2006). Several studies pointed out a similar TOR domain structure in all eukaryotes. The Huntington, Elongation Factor 3, PR65/A, TOR (HEAT) repeats domains consist of approximately 20 HEAT motifs, each of which is ~40 residues that form a pair of interacting antiparallel  $\alpha$ -helices (Andrade and Bork, 1995; Perry and Kleckner, 2003). The HEAT repeats occupy the N-terminal half of TOR and are the binding region for subunits of the TOR complexes (Wullschleger *et al.*, 2005). The central Focal Adhesion Targeting (FAT) domain contains ~500 residues and the extreme C-terminal FRAP-ATM-TRRAP-C-terminal (FATC) domain ~35 residues, flanking the FKBP-rapamycin binding (FRB) and the kinase domains, are always paired and found in all PIKK family members (Alarcon *et al.*, 1999; Bosotti *et al.*, 2000; Dames *et al.*, 2005). The FRB domain (~100 residues) is the FKBP-rapamycin-binding region (**Figure 1.1 A**).

TOR kinase is the focus of extensive research due to its role in health, diseases, cancer and aging. In yeast and mammals, its function is performed through two-multi-protein complexes, named TORC1 and TORC2, which differ in their complex assembly, sensitivity to rapamycin and functions. TORC1, formed by TOR, RAPTOR and LST8; is related mainly to ribosome biogenesis, translation, transcription, metabolism, inhibition of autophagy and protein degradation processes. In contrast, TORC2, assembled by TOR, RICTOR, LST8 and Sin1; is responsible to control cytoskeleton organization and cell cycle progression (**Figure 1.1 B**) (Laplane and Sabatini, 2012). TORC1 is inhibited through the formation of a ternary complex among rapamycin, the immunophilin FKBP12 and the FRB domain of TOR. This complex is the most characterized due to its role in integrating environmental factors, metabolism, and cell growth (Wullschleger *et al.*, 2006).

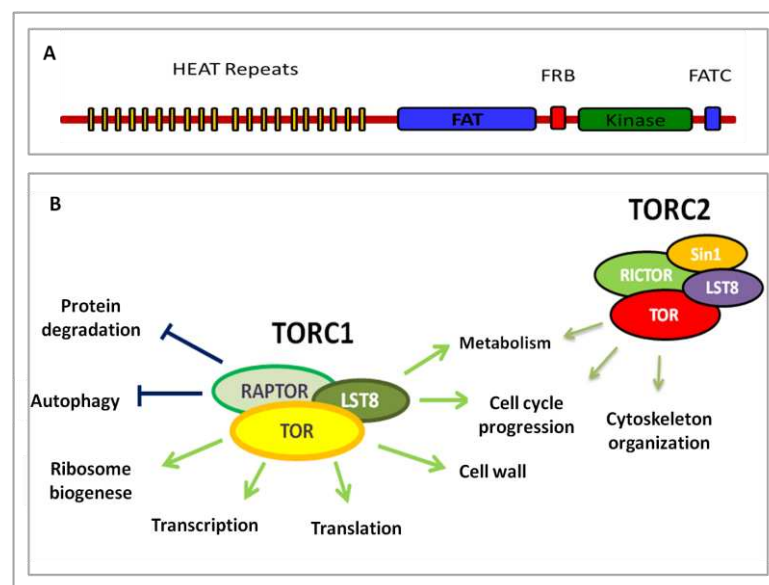


**Figure 1.1 - Target of rapamycin in eukaryotes. In *Arabidopsis* there is no evidence proving the existence of the TORC2.**

(A) Organization of domains of the components of TOR; (B) TORC1 and TORC2 complexes and their functions.

The *Arabidopsis thaliana* genome contains a single copy of the gene TOR, two copies of RAPTOR (regulatory associated protein of TOR) that are expressed, and two putative LST8 (G – protein  $\beta$ -subunit-like/lethal with Sec thirteen 8) genes, of which only one (LST8-1) is significantly expressed (Garrett *et al.*, 2005; Ren *et al.*, 2011; Moreau *et al.*, 2012). Although all essential genes are present in *Arabidopsis* genome, the treatment of plants with rapamycin does not lead to growth arrest as it has been observed for other eukaryotes. This is due to the substitution of essential amino acids in

the sequence of the immunophilin FKBP12 of *Arabidopsis* required for interaction between rapamycin and TOR. However, rapamycin could arrest plant growth when applied in concentrations 100-fold higher than the ones used in yeast and mammals (Xiong and Sheen, 2012).

Despite the different strategies of plants for their growth and development, the function of TOR in coupling nutrients and energy availability with other environmental signals to coordinate growth, development and survival seems to be conserved in yeast, animals and plants. Generally, in *Arabidopsis*, TOR expression levels correlate with the growth of roots and shoots, cellular size and seed production (Deprost *et al.*, 2007). Furthermore, TOR loss-of-function T-DNA insertion lines displayed embryonic lethality and arrest of endosperm development at the torpedo stage, pointing TOR as an essential protein (Menand *et al.*, 2002).

Transgenic lines with conditional repression of TOR through interference RNA or artificial micro RNA and rapamycin-sensitive transgenic lines expressing yeast FK506 Binding Protein have been used to overcome the lethality of knockout mutants (Deprost *et al.*, 2007; Ren *et al.*, 2012; Caldana *et al.*, 2013; Xiong *et al.*, 2013). With the aim of inhibiting the TOR pathway more efficiently than rapamycin, new mammalian TOR-specific inhibitors (asTORis) have been developed (Zhang *et al.*, 2011). These new TOR inhibitors are ATP competitive because they target the ATP-binding site of the kinase domain (Dowling *et al.*, 2010). They have been selected for their specificity by *in vitro* kinase assays with a wide range of protein kinases (Garcia-Martinez *et al.*, 2009; Thoreen *et al.*, 2009; Yu *et al.*, 2009; Chresta *et al.*, 2010; Liu *et al.*, 2010; Yu *et al.*, 2010; Liu *et al.*, 2011). Montané and Menand (2013) have shown the dose-dependent effect of first (KU63794, Torin1, WYE-354) and second-generation inhibitors (AZD-8055, Torin2, WYE-132) on *Arabidopsis* root growth. Second-generation inhibitors were developed to improve pharmacodynamics of first-generation inhibitors (Chresta *et al.*, 2010; Yu *et al.*, 2010; Liu *et al.*, 2011). Each asTORis used in that work inhibited root growth at concentrations ranging from 0.1 up to 10  $\mu$ M (Garcia-Martinez *et al.*, 2009; Thoreen *et al.*, 2009; Yu *et al.*, 2009; Chresta *et al.*, 2010; Yu *et al.*, 2010; Liu *et al.*, 2011). However, second-generation molecules were about ten times more efficient in inhibiting growth than the first-generation inhibitors and clearly inhibited root growth at concentrations below 1  $\mu$ M in less than 50 hours after treatment. AZD-8055 was shown to inhibit the growth of two ecotypes of *A. thaliana*, suggesting that asTORis impair growth independently of the ecotype. The use of

chemical TOR inhibitors has opened new perspectives to dissect the TOR function in plants without the need of creating transgenic lines. Despite the limitations concerning the use of TOR-silenced lines to characterize this pathway in plants, these lines can still be used in a wide range of assays to determine TOR-function in plants depending on the biological question to be answered.

The major conserved processes involving the TOR pathway among organisms are the ones related to the control of protein synthesis at multiple levels. TOR regulates rRNA transcription through its kinase domain. Chromatin immunoprecipitation studies demonstrated that *Arabidopsis* TOR directly binds to the 45S rRNA promoter and the 5' untranslated region via the Leu-zipper sequence within the HEAT repeat domain of TOR to directly regulate 45S rRNA transcription (Ren *et al.*, 2011). The transcription of a large number of genes encoding ribosomal proteins (RPs) are similarly regulated by TOR in yeast, *Arabidopsis*, and mouse, suggesting another conserved TOR function that is central to ribosome biogenesis (Martin *et al.*, 2004; Huber *et al.*, 2009; Chauvin *et al.*, 2013; Xiong *et al.*, 2013). The S6K is a well-known target of TOR. TOR phosphorylates and activates S6K, which phosphorylates the ribosomal protein S6. Ribosomal protein S6 is a key component of the 40S ribosomal subunit, integrating t-RNA recruitment to mRNA and translation initiation factors, and thus regulating translation of mRNAs (Ruvinsky and Meyuhas, 2006). S6 was the first identified ribosomal protein target of inducible phosphorylation by growth factors and also by the RPS6 kinase (S6K) (Krieg *et al.*, 1988; Franco and Rosenfeld, 1990; Ruvinsky and Meyuhas, 2006).

In conditions where nutrients and energy are available to promote protein synthesis and growth, TOR acts inhibiting the autophagy process. Autophagy is responsible for directing cytoplasmic components to vacuoles or lysosomes to be degraded to generate precursors during starvation periods and in stress conditions. TORC1 is a key inhibitor of autophagy, regulated by multiple upstream factors including oxygen, amino acids, glucose, and growth factors. In yeast, multiple genes essential for autophagy (referred to as ATG genes) act downstream of TOR. ATG proteins are conserved in mammals and function to induce the generation, maturation, and recycling of autophagosomes. In *Arabidopsis*, the down-regulation of TOR expression activates constitutively the autophagy process (Liu and Basham, 2010). In *Chlamydomonas reinhardtii*, TOR inhibition by rapamycin similarly induces autophagy (Pérez-Pérez *et al.*, 2010). These results demonstrate that TOR is a conserved negative

regulator of autophagy not only in photosynthetic species, but also in mammals and yeasts.

Several lines of evidence also point to a fundamental role of TOR on carbon (C) and nitrogen (N) balance and its action as an essential regulator of central energy metabolism (Wullschleger *et al.*, 2006; Castrillo *et al.*, 2007; Düvel *et al.*, 2010; Ren *et al.*, 2012; Caldana *et al.*, 2013; Xiong *et al.*, 2013). In *Arabidopsis*, the reduction of gene expression levels or kinase activity of TOR leads to an accumulation of starch, triacylglycerides (TGA), amino acids, intermediates of TCA and secondary metabolites (Ren *et al.*, 2012; Caldana *et al.*, 2013; Xiong *et al.*, 2013). Additionally, TGA excess phenotype mainly of polyunsaturated long chain was also observed in TOR-silenced plants (Caldana *et al.*, 2013) and represents another form to accumulate the excess of C and energy (Li-Beisson *et al.*, 2013).

Cell wall can serve as a short and long-term structure to store C. However, cell wall is a C sink and TOR modulates its biogenesis. Leiber *et al.* (2010) proposed a mechanism in which TOR participates in cell wall formation. The *lrx1* mutant develops abnormal root hairs since it is an extracellular protein involved in cell wall formation in this tissue (Baumberger *et al.*, 2001; Baumberger *et al.*, 2003a, 2003b). *rol5* mutant has been identified as a suppressor of *lrx1* (Leiber *et al.*, 2010). The functionally similar ROL5 homolog in yeast was shown to affect TOR signaling. Inhibition of TOR signaling in that work by using rapamycin led to suppression of the *lrx1* mutant phenotype and caused changes to galactan/rhamnogalacturonan-I and arabinogalactan protein components of cell walls that were similar to those observed in the *rol5* mutant.

The participation of TOR on C metabolism was also shown by transgenic lines with reduced TOR and LST8 expression that accumulate high amounts of starch (Moreau *et al.*, 2012; Caldana *et al.*, 2013; Dobrenel *et al.*, 2013). Starch is the main C storage compound in plants and its abundance correlates negatively with growth (Sulpice *et al.*, 2009). The accumulation of starch in TOR-silenced plants is reminiscent of the fact that the repression of TORC1 in yeast and mammals leads to accumulation of glycogen, an analogous form of starch (Schmelzle *et al.*, 2004; Cornu *et al.*, 2013). Different from animals and yeasts, the influence of TOR kinase on C metabolism in plants is not yet elucidated.

## 1.2 - Carbon metabolism in plants

Autotrophic organisms are able to transform light energy into chemical energy through the photosynthetic process. In the presence of light, photoassimilates are usually partitioned into sucrose and transitory starch in the chloroplasts, being the percentage of each compound variable among plant species. During the night, starch is remobilized to sustain metabolism and plant growth (Kotting *et al.*, 2010; Santelia and Zeeman, 2011). The synthesis and degradation of transitory starch are finely coordinated with the day length and the C anticipated necessity for plants in the night period. Starch is also a long-term storage compound and is accumulated in heterotrophic organs such as seeds, roots and tubers (Sonnewald and Kossmann, 2013).

Starch is composed of two types of polymers, amylose and amylopectin, which are assembled in insoluble crystalline granules and are species-specific in number, form and size (Zeeman *et al.*, 2010; Sonnewald and Kossmann, 2013). Amylose is a linear chain of glucose residues linked via  $\alpha$ -1,4 bonds, while amylopectin is a branched polymer of glucose linked through  $\alpha$ -1,6 bonds.

The pattern of starch degradation is essentially linear and starch is consumed in almost its totality during the night (Gibon *et al.*, 2004). In addition, the rate of starch degradation can immediately adjust to an unexpected early onset of the night, suggesting that *Arabidopsis* plants are able to measure the amount of starch in the leaf at the end of the day and accurately anticipate the length of the forthcoming night (Graf *et al.*, 2010). Moreover, the timing of starch degradation is linked to the circadian clock because a mutant lacking the LHY and CCA1 clock components exhausted its starch at the dawn anticipated and become C starved at night (Graf *et al.*, 2010).

Due to its importance, fine-tuning disturbs in the starch synthesis and degradation pathways affect the metabolism, growth and development of plants (Caspar *et al.*, 1985; Lin *et al.*, 1988; Stitt and Zeeman, 2012). During dark periods, after leaf emergence, growth is diminished when the amount of starch is low. This is followed by rapid and massive changes in metabolism, gene expression and inhibition of growth until one or two hours of the next day (Pantin *et al.*, 2011). Conversely, incomplete remobilization of starch leads to a reduction in biomass as it sequesters C that could be used to promote growth of roots and leaves (Weise *et al.*, 2012).

Plants grown in short-day conditions partition more C as starch than plants grown in long days. It means that the longer is the period without light, the higher is the

amount of starch storage to provide energy during the period of darkness (Zeeman *et al.*, 2007). Mutations affecting starch metabolism have been important to characterize the synthesis and degradation pathways as well as the mechanisms that control these processes. Mutations related to starch metabolism resulted in disturbs and diminution of growth showing the great importance of the daily turnover of this polymer (Zeeman *et al.*, 2007).

### 1.3 - Biosynthesis of starch

The biosynthesis of starch occurs in the presence of light in chloroplasts of leaves and in amyloplasts of organs without chlorophylls. The production of starch is finely regulated at several levels to control the flow of C from the Calvin-cycle and the amount of stored starch depends on environmental conditions, mainly the day length (Zeeman *et al.*, 2007). According to Sttit and Zeeman (2012), the conversion of photosynthetic products in transitory starch is around 30-50% in *Arabidopsis*.

Starch synthesis occurs through the action of several enzymes, being adenosine diphosphate glucose (ADP-glucose) the main substrate of starch synthases, which are responsible to catalyze the polymerization of glucose molecules (Sonnewald and Kossmann, 2013). It has been accepted that the ability of plants to synthesize starch granules evolved from an ancestral competence to produce glycogen, a polymer of glucose simpler, branched and soluble (Ball and Morell, 2003). For the occurrence of polymerization and branching of the starch granules it is necessary a primer in which starch synthases are able to act. However, there is no confirmed evidence for the ability of starch synthases to produce glycan chains from ADP-glucose, being necessary the presence of an acceptor of glycan. Possibly, the beginning of starch granule formation in plants is under genetic control, different from mammals and yeasts, where the molecules of glycogen are initiated through the glycogenin enzyme without the need of a primer acceptor (Zeeman *et al.*, 2007).

ADP-glucose is directly linked to the Cavin-Benson cycle through several enzymatic steps. The trioses phosphates produced in this pathway are substrates for aldolases, originating fructose-1,6-bisphosphate, which is then dephosphorylated by fructose-1,6-biphosphatase in fructose-6-phosphate. This last sugar is converted in glucose-6-phosphate and subsequently in glucose-1-phosphate through the action of



phosphoglucose isomerase (PGI) and phosphoglucomutase (PGM), respectively (Stitt and Zeeman, 2012).

ADP-glucose pyrophosphorylase (AGPase) catalyzes the first committed step in the pathway of starch synthesis. The higher plant enzyme is a heterotetramer that contains two regulatory large (51 kD) and two slightly smaller (50 kD) catalytic subunits. AGPase forms ADP-glucose from glucose-1-phosphate and ATP, releasing inorganic pyrophosphate (PPi). Starch synthases (SSs) catalyze reactions using ADP-glucose to build  $\alpha$ -(1,4)-linked linear glucosyl chains. Branching enzymes (BEs) are responsible to introduce branch linkages by cleaving an internal  $\alpha$ -(1,4) linkage and creating a new  $\alpha$ -(1,6) linkage by transferring the released reducing end to a C6 hydroxyl. Starch-debranching enzymes (DBEs) hydrolyze branches (**Figure 1.2**). Multiple SS, BE, and DBE isoforms exist in all plant species, and their strong evolutionary conservation suggests that each isoform class functions uniquely in starch metabolism. Five distinct SS classes are known in all plants based on amino acid sequence similarities: granule-bound SS (GBSS), SSI, SSII, SSIII, and SSIV/V. Genetic analyses in plants that accumulate storage starch indicate that at least three of the SS classes are essentials in starch biosynthesis: GBSS (Shure *et al.*, 1983; Klösigen *et al.*, 1986); SSIII (Gao *et al.*, 1998; Cao *et al.*, 1999); and SSII (Craig *et al.*, 1998; Morell *et al.*, 2003; Zhang *et al.*, 2004).

In storage organs, such as endosperm of seeds and potato tuber, the C for starch synthesis is provided from the cytoplasm. It has been accepted that depending on the species, glucose-6-phosphate or glucose-1-phosphate could be imported for the amyloplast through the action of a transporter of hexose phosphates (Sonnewald and Kossmann, 2013).

It has been questioned whether there is only one starch biosynthetic pathway because *pgm1* mutant (absence of phosphoglucomutase) and *adg1* (absence of the small subunit of AGPase -APS1) are able to produce starch, even in small quantities when compared to wild type. This implies that probably in every mutant the metabolism of chloroplast or importation are sources for precursors of starch synthesis. Importation of glucose-1-phosphate for the chloroplast might explain any content of starch present in the *pgm1* mutant. The content of starch found in the *adg1* mutant can be due to a residual activity of AGPase, eventually enough for the synthesis of starch even in low quantities. Despite the possibility of new routes for starch synthesis, the one mediated by AGPase is the most important in *Arabidopsis* (Stitt and Zeeman, 2012).

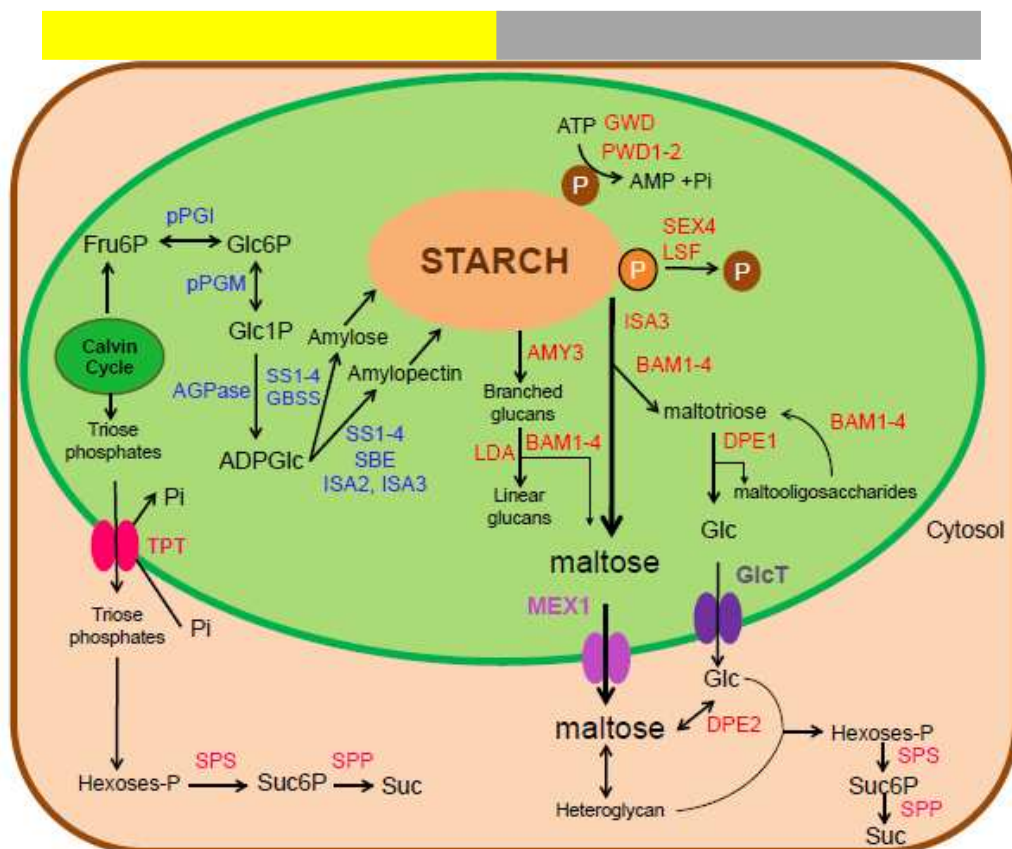


Figure 1.2 – Illustrative scheme of the pathway of starch synthesis and degradation in leaves of *Arabidopsis thaliana*. Adapted from Stitt and Zeeman, 2012.

#### 1.4 - Starch degradation

The degradation of transitory starch in leaves occurs during the night and the main products exported from chloroplast are maltose and glucose. Glucose-1-phosphate may be generated and possibly used in chloroplast or exported to cytosol (Stitt and Zeeman, 2012). The first steps for starch mobilization are catalyzed by the enzyme glucan water dikinase (PWD) and phosphoglucan water dikinase (PWD), which phosphorylate glucose residues at C6 and C3 positions, respectively. PWD is able to act only after the phosphorylation performed by GWD. Subsequently to the action of these enzymes, a destabilization in the granule surface occurs facilitating the binding of other hydrolases.  $\beta$ - amylases (BAMs) are responsible to hydrolyze  $\alpha$ -1,4 glycosidic bonds between glucose residues generating maltose, the main product of starch breakdown in *Arabidopsis*. The branching points in starch structure are hydrolyzed by debranching enzymes,  $\alpha$ -amylases and pululanases (Stitt and Zeeman, 2012; Sonnewald and Kossmann, 2013).

In *Arabidopsis*, the generated maltose is exported from plastids through a maltose transporter (MEX1) and further metabolized by the cytosolic deproportionating enzyme (DPE2), producing glucose and heteroglycans that serve as intermediates for C storage (**Figure 1.2**) (Sonnewald and Kossmann, 2013). The exo-amylolytic activity is impaired by phosphate groups, thus phosphate residues are removed from starch by two specific phosphatases, starch excess 4 (SEX4) and like sex four2 (LSF2) to ensure complete degradation. SEX4 hydrolyzes phosphate bonds at both C3 and C6 positions, while LSF2 preferentially breaks bonds at C3 positions in glucose molecules. Therefore, during the starch degradation process the granule surface is primarily destabilized by phosphorylation, subsequently degraded by hydrolytic enzymes and then finally dephosphorylate by SEX4 and LSF2 (Sonnewald and Kossmann, 2013).

### 1.5 - Regulation of starch metabolism

Studies related to starch synthesis and its regulation were primarily focused in its integration with the Calvin-Benson cycle and sucrose synthesis. During light periods when photosynthesis is supposed to occurs, photoassimilates are produced. However, the syntheses of starch and sucrose are competing reactions. In other words, the synthesis of sucrose down-regulates starch synthesis and vice-versa (Taiz and Zeiger, 2010). The most important factors controlling the partition of fixed C between starch and sucrose synthesized in the stroma of chloroplasts and cytosol, respectively, are trioses phosphates generated after photosynthetic process and orthophosphate (Pi) (**Figure 1.3**).

In the inner membrane of the chloroplast, there is an integral membrane protein known as triose phosphate translocator. The phosphate translocator catalyzes the movement of Pi and triose phosphate in opposite directions between chloroplast and cytosol. A low concentration of Pi in the cytosol limits the export of triose phosphate from the chloroplast through the translocator, thereby promoting the synthesis of starch. Conversely, an abundance of Pi in the cytosol inhibits starch synthesis within the chloroplast and promotes the export of triose phosphate into the cytosol, where it is converted to sucrose (Flügge *et al.*, 1989).

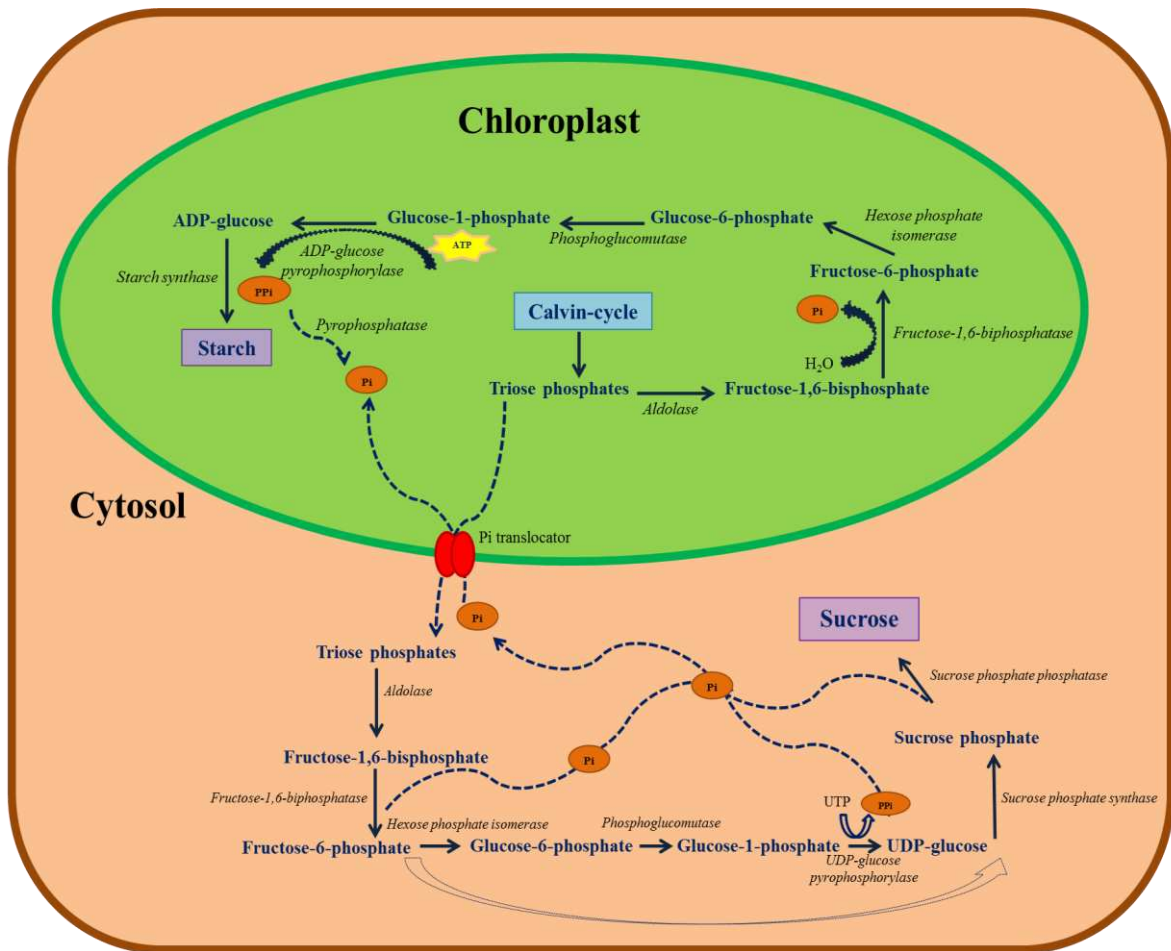


**Figure 1.3 - Syntheses of starch and sucrose are competing processes that occur in chloroplast and cytosol, respectively.**

When the cytosolic Pi concentration is high, chloroplast triose phosphate is exported to the cytosol via the Pi translocator in exchange for Pi, and sucrose is synthesized. When the cytosolic Pi concentration is low, triose phosphate is retained. Adapted from Taiz and Zeiger, 2010.

Pi and triose phosphate control the activity of several regulatory enzymes in the sucrose and starch biosynthetic pathways. The chloroplastic enzyme AGPase is one of the most important in the regulation of starch synthesis from glucose-1-phosphate. This enzyme is stimulated by 3-phosphoglycerate and inhibited by Pi. A high concentration ratio of 3-phosphoglycerate to Pi is typically found in illuminated chloroplasts that are actively synthesizing starch. Reciprocal conditions prevail in the dark (Zeeman *et al.*, 2007; Taiz and Zeiger, 2010).

Fructose-2,6-bisphosphate is a key molecule that controls the increase and decrease of sucrose synthesis in the light and dark, respectively. It is located in the cytosol in low concentrations and exerts a regulatory effect on the cytosolic interconversion of fructose-1,6-bisphosphate and fructose-6-phosphate (**Figure 1.4**). Increased cytosolic fructose-2,6-bisphosphate is associated with decreased rates of

sucrose synthesis because fructose-2,6-bisphosphate is a powerful inhibitor of cytosolic fructose-1,6-bisphosphatase and an activator of the pyrophosphate-dependent (PPi-linked) phosphofructokinase.

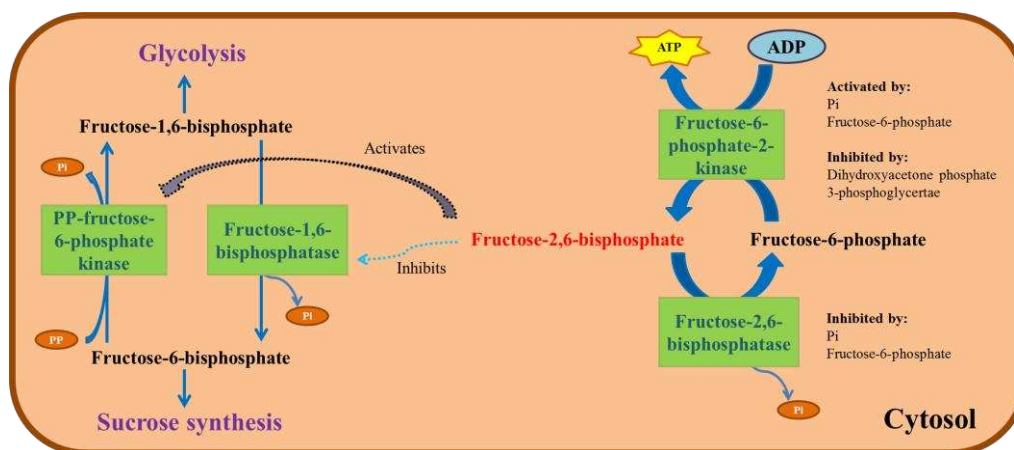


**Figure 1.4 - Regulation of the cytosolic interconversion of fructose-6-phosphate and fructose-1,6-bisphosphate.** The regulatory metabolite fructose-2,6-bisphosphate regulates the interconversion by inhibiting the phosphatase and activating the kinase, as shown. The synthesis of fructose-2,6-bisphosphate itself is under strict regulation by the activators and inhibitors shown in the figure. Adapted from Taiz and Zeiger, 2010.

Fructose-2,6-bisphosphate is synthesized from fructose-6-phosphate by a special fructose-6-phosphate 2-kinase and is degraded specifically by fructose-2,6-bisphosphatase. Recent evidence suggests that, as in animal cells, both plant activities reside on a single polypeptide chain. The kinase and phosphatase activities are controlled by  $P_i$  and triose phosphate.  $P_i$  stimulates fructose-6-phosphate 2-kinase and inhibits fructose-2,6-bisphosphatase, whereas triose phosphate inhibits the 2-kinase. Consequently, a low cytosolic ratio of triose phosphate to  $P_i$  promotes the formation of fructose-2,6-bisphosphate, which in turn inhibits the hydrolysis of cytosolic fructose-1,6-bisphosphate and slows down the rate of sucrose synthesis. A high cytosolic ratio of triose phosphate to  $P_i$  has the opposite effect (Neuhaus and Stitt, 1990; Scott *et al.*, 1995).

Light regulates the concentration of these activators and inhibitors through the reactions associated with photosynthesis and thereby controlling the concentration of fructose-2,6-bisphosphate in the cytosol. The glycolytic enzyme phosphofructokinase also functions in the conversion of fructose-6-phosphate to fructose-1,6-bisphosphate, but in plants it is not appreciably affected by fructose-2,6-bisphosphate. The activity of phosphofructokinase in plants appears to be regulated by the relative concentrations of ATP, ADP, and AMP (Taiz and Zeiger, 2010).

The synthesis of starch occurs when C fixation exceeds sucrose synthesis (Stitt and Zeeman, 2012). When the rate of sucrose synthesis exceeds the demand of sink organs, it is believed that sucrose accumulates in the mesophyll cells. High levels of sucrose serve as a signal to stimulate starch synthesis and to adjust the photosynthetic activity for other needs of the plant (Sonnewald and Kossman, 2013).

The regulation of AGPase also occurs through the ferredoxin-thioredoxin system. The inactivation of AGPase by this system takes place when sulfur groups of cysteine residues from the C-terminal domain of the small subunit become oxidized, forming a disulphide bond between two subunits. In light periods or in the presence of sugar, mainly sucrose, the disulphide bond is broken resulting in activation of AGPase (Zeeman *et al.*, 2007; Stitt and Zeeman, 2012). The activated and inactivated states of the enzyme change during the day/night cycle being partially activated along the day and deactivated at night. This mechanism prevents the flow of metabolites in the direction of starch synthesis overnight (Zeeman *et al.*, 2007). The degree of AGPase activation via reduction seems to be sensitive to metabolic changes. Whereas AGPase light-dependent activation is mediated by the ferredoxin-thioredoxin system, the sucrose-dependent activation is performed by the double function of NADPH-thioredoxin (Stitt and Zeeman, 2012).

AGPase has been proposed as a target of the metabolite trehalose-6-phosphate (T6P), as incubation of isolated chloroplasts with up to 1 mM T6P promoted the redox activation of this enzyme (Kolbe *et al.*, 2005). In addition, *Arabidopsis* mutants that constitutively overexpress the enzyme trehalose-phosphate synthase (TPS), and thus possess high T6P levels, showed greater redox activation of AGPase and higher starch levels in comparison to control plants (Schluepmann *et al.*, 2003; Kolbe *et al.*, 2005; Winkler *et al.*, 2012). Due to the fact that T6P acts as a sucrose signaling molecule to regulate several steps of metabolism, it could provide an explanation for the linkage between starch and sucrose, possibly indicating the C status of the plant (Lunn *et al.*, 2006; Stitt and Zeeman, 2012; Yadav *et al.*, 2014).

However, there is conflicting evidence concerning the effect of T6P on the redox activation status of AGPase and its role in regulating starch synthesis. Although it was shown that the redox status of AGPase in *Arabidopsis* rosettes changes in parallel with diurnal fluctuations in sucrose content and T6P (Lunn *et al.*, 2006), this might be an independent response to sucrose as plants carrying an ethanol-inducible TPS construct that generated a 2 to 3-fold increase in the level of T6P did not support this hypothesis

(Martins *et al.*, 2013). However, Figueroa *et al.* (2016) showed that increased T6P levels in these induced plants were accompanied by a transient 20-30% decrease in sucrose content but only a slight increase in starch content was observed in the induced plants compared to the control. Furthermore, the estimated cytosolic concentration of T6P in the light is reported to be substantially below the range of concentrations used by Kolbe *et al.* (2005). Finally, some studies called into question whether the redox modulation of AGPase is really relevant for the starch synthesis and in which conditions. Mutagenesis of a residue that impairs the formation of the disulphide bound had surprisingly little effect on the rate of starch synthesis, except under short-day conditions at low irradiance (Hädrich *et al.*, 2012). Moreover, post-translational redox modification of AGPase in response to light was shown not to be the main determinant of fine regulation of transitory starch accumulation in *Arabidopsis* (Li *et al.*, 2012). In conclusion, AGPase can exert negligible control over flux through the pathway of starch synthesis in *Arabidopsis* depending on the growth condition and there is little evidence that T6P on its own could play a dominant role in regulating the redox status of AGPase.

In *Arabidopsis*, T6P is a strong inhibitor of SNF1-related kinase1 (SnRK1), a central integrator of stress and energy signalling, which regulates anabolism and catabolism. Nunes *et al.* (2013) uncoupled tissue sugar content from growth and demonstrated a correlation between T6P and sucrose levels under sink limited conditions in several treatments, and also a strong increase in starch content. In addition, elevated T6P levels led to a decrease in SnRK1 activity assayed *in vitro*. It is hypothesized that high levels of sucrose would lead to SnRK1 inhibition by T6P and thereby starch synthesis would outperform starch degradation leading to a substantial increase in starch content. This has been shown in transgenic *Arabidopsis* plants with elevated T6P content, which showed an increased starch level (Zhang *et al.*, 2009).

The precise timing of starch degradation has implicated the circadian clock in the regulation of degradation. Transcriptional analyses of genes involved in starch breakdown showed high and coordinate daily changes, which are directed by the circadian clock. The rate of starch degradation is immediately diminished or increased when plants are placed in anticipated night or extended day, respectively (Lu and Sharkey, 2005; Graf *et al.*, 2010; Sulpice *et al.*, 2014). These results show that the rate of starch breakdown during the night is influenced by the previous photoperiod length (Zeeman and Smith, 2007).

The mechanisms controlling starch degradation are not completely understood but several evidences of transcriptional control, feedback inhibition, redox regulation and protein phosphorylation have been emerged recently. It is known that interruption of exportation or addition of sugars in leaves growing in darkness result in low rate of starch degradation. This could involve both stimulus for starch synthesis or inhibition of its degradation (Stitt and Zeeman, 2012). There are many post-translational mechanisms that possibly regulate enzymes of starch degradation. First, accumulation of intermediates of starch pathway could impair the release of glucan from starch granules. Furthermore, the enzymes involved in starch breakdown are regulated by phosphorylation. The mutation in two phosphatases (SEX4 – protein-tyrosine phosphatase kinase interaction sequence and DSP4 – dual-specificity phosphatase 4) leads to a reduction in starch degradation and consequently a starch excess phenotype (Sokolov *et al.*, 2006; Kötting *et al.*, 2009). Plants grown in short-day conditions, low-light intensities and low CO<sub>2</sub> concentration synthesize proportionally higher quantities of starch during light periods and degrade this polymer slowly overnight. Consequently, a few quantity of starch is still found at the end of night (Matt *et al.*, 2001; Gibon *et al.*, 2004). Since plants are subjected to continuous changes in C supply it is necessary to adjust their daily starch turnover with the diminution of C used in respiration and growth processes. Mutants of starch biosynthesis pathway illustrate the importance of the balance between availability of C sources during the day from photosynthesis and during the night from starch breakdown. These mutants are not able to grow in a light/dark cycle because the content of C becomes limited along night, leading to growth inhibition (Sulpice *et al.*, 2009).

## **1.6 - Evidences for the influence of TOR on starch metabolism**

All organisms, including plants, have developed the capacity to ameliorate the use of available nutrients and adapt their metabolism for growth and survival. Plants are sessile and subjected to different environmental conditions, and thus need to be able to monitor precisely sudden environmental changes to guarantee their survival and adaptation, maintaining growth and biomass production. As in other eukaryotes, TOR has emerged as one of the most important signalling pathways in plants, responsible for integrating external signals with metabolic adaptations and growth (Dobrenel *et al.*, 2013).



Several pieces of evidence suggest that TOR has an influence on C and N metabolism. In *C. reinhardtii*, N starvation leads to accumulation of starch and triacylglycerides (TGAs) (Ball *et al.*, 2011). It has been reported that plants affected on N assimilation accumulate higher content of starch (Dobrenel *et al.*, 2013). These results point clearly to a starch control in response to N availability. In N starvation conditions, growth is reduced and the major part of C is redirected to the pathway of starch instead of being used in cell wall synthesis or energy production (Dobrenel *et al.*, 2013). Conditional silencing of TOR gene in *A. thaliana* using micro artificial RNA induced for estradiol showed a starch and TGA excess phenotype (Caldana *et al.*, 2013). Transgenic lines with reduced LST8 (TORC1 component) expression also accumulate high amounts of starch (Moreau *et al.*, 2012).

Inhibition of TOR activity leads to glycogen accumulation in muscular cell of mammals and yeasts (Schmelzle *et al.*, 2004; Cornu *et al.*, 2013). Under normal growth conditions, TORC1 phosphorylates TAP42 that dephosphorylates the transcription factor Msn2p. In contrast, under starvation, TOR is inactivated and precludes TAP42 phosphorylation, allowing Msn2p phosphorylation and consequently, translocation to the nucleus. In the nucleus, Msn2p binds to stress response element (STRE) regulatory sequence located in the promoter region of glycogen synthesis-encoding genes resulting in a glycogen excess phenotype (François *et al.*, 2012). In muscular cells of mammals, PKB/AKT proteins are responsible to inhibit the action of glycogen synthase kinase3 $\beta$  (GSK3 $\beta$ ) in cells where TOR is active. In contrast, repression of TOR leads to phosphorylation of PKB/AKT in 308 threonine and 473 serine residues. GSK3 $\beta$  is phosphorylated at 9 serine residues becoming inactive, and consequently, releasing the active form of glycogen synthase which, promotes glycogen synthesis and accumulation (Bentzinger *et al.*, 2008). Furthermore, it has also been reported that the gene encoding for the glycogen phosphorylase, responsible for the glycogen breakdown into glucose, is down-regulated (**Figure 1.5**) (Bentzinger *et al.*, 2008). Opposite to muscular and yeast cells, in liver the glycogen excess phenotype is not observed when the TOR pathway is disrupted. Non-starved liver cells reduce blood glucose levels via consumption (glycolysis) or conversion of glucose to glycogen (glycogenesis) or triglyceride (lipogenesis). Genetically modified mice with defective mTOR presents decreased glycogen content. Lipogenesis *in vitro* is activated through the transcription factor sterol regulatory element-binding protein (SREBP). mTORC1 mediates maturation of SREBP-1 in an S6K1-dependent manner to stimulate *de novo* lipid synthesis. However,

mTORC1 also stimulates SREBP-1 expression in an S6K-independent manner, which involves the mTORC1 substrate phosphatidic acid phosphatase lipin-1, a negative regulator of SREBP-1 activity. In response to nutrients and growth factors, mTORC1 directly phosphorylates lipin-1, preventing its translocation into the nucleus, thereby allowing SREBP transcriptional activity (Cornu *et al.*, 2013).

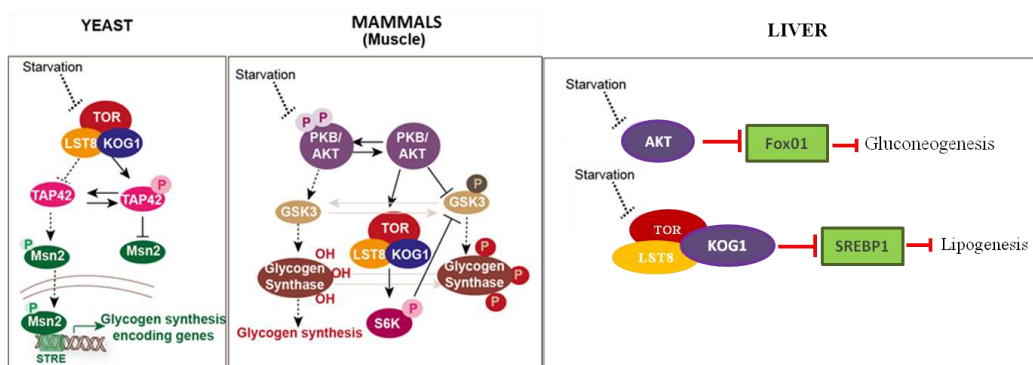


**Figure 1.5 – Repression of TOR gene by rapamycin leads to glycogen excess phenotype in yeast and in muscle mammal cells but the opposite is observed for liver cells.**

The participation of TOR on glycogen metabolism in yeast and mammals has been established at the transcriptional level as exposed in the scheme above. Adapted from Bentzinger *et al.* (2008) and François *et al.* (2012).

However, it remains to be elucidated the participation of this pathway on starch metabolism in plants. Since the metabolism of starch is very complex, compartmentalized and interacts with other pathways, this polymer is subject to several levels of regulation. We are currently investigating some possibilities in which TOR could play a role in modulating directly or indirectly the starch metabolism. It is not yet known whether the starch excess phenotype in TOR-silenced plants is due to increased starch synthesis, diminished degradation or both. Furthermore, maximal catalytic activity of key enzymes in TOR-impacted plants and a study considering short-term TOR-repression have never been assessed to identify putative mechanisms of the starch excess phenotype. In addition, some studies pointed out to the possibility of a link between starch, sucrose and the levels of T6P, because this latter molecule influences the relative amounts of sucrose and starch that accumulate in leaves during the day, and regulates the rate of starch degradation at night to match the demand for sucrose (Figuerola *et al.*, 2016). It has also been proposed that T6P influences plant growth and development via inhibition of the SnRK1. Therefore, there are many possibilities in which TOR could modulate primary metabolism and it is expected that the results obtained in this work may contribute to a better understanding of the crosstalk between this pathway and C and storage compounds metabolism in *A. thaliana*.

## 2 - Objectives

The main goal of this study was to characterize the influence of the Target of Rapamycin (TOR) kinase on starch metabolism in the plant model *Arabidopsis thaliana*. For this purpose, specific objectives were established:

- Development of a hydroponic system to facilitate the administration of AZD-8055 (TOR-inhibitor) to plants;
- Investigation of starch accumulation kinetics during the diel cycle to determine if the starch excess phenotype described in previous works was due to increased synthesis, diminished degradation or both;
- Measurement of metabolites related to starch and sucrose metabolism;
- Enzymatic assays, gene expression and western blot analyses of AGPase, the regulatory enzyme of starch synthesis;
- Determination of cellular redox potential;

### **3 - Material and Methods**

All experiments in this work were performed at the Brazilian Bioethanol Science and Technology Laboratory (CTBE) in the group of Molecular Plant Physiology, located in Campinas – São Paulo in 2015.

#### **3.1 - Chemicals**

All chemicals and reagents were obtained from Sigma-Aldrich Brasil Ltda, Merck Brasil or Roche Diagnóstica Brasil Ltda, unless stated otherwise. Enzymes for starch and glutathione measurements were purchased from Roche Diagnóstica Brasil Ltda and Sigma-Aldrich Brasil Ltda, respectively. Molecular kits were obtained from Qiagen Biotecnologia Brasil Ltda. Affinity purified rabbit antibodies raised against the *A. thaliana* AGPase small subunit and anti-rabbit IgG horse radish peroxidase conjugated were obtained from Agrisera (Sweden).

#### **3.2 - Plant material and growth conditions**

Seeds of *Arabidopsis thaliana* ecotype Columbia (Col-0) were surface sterilized under agitation using 70% ethanol for 3 minutes, subsequently incubated for 5 minutes in a solution of 10% sodium hypochlorite containing Tween20, followed by 6 washes with autoclaved distilled water. After sterilization, seeds were stratified at 4°C in the dark for 5 days to synchronize germination and placed at the hydroponic system. Seedlings were cultivated in a growth chamber with 75% of humidity, 150  $\mu\text{mol m}^{-2} \text{s}^{-1}$  of irradiance, 12 h day (21°C)/ 12 h night (19°C). The growth of the seedlings was accompanied until the stage of 1.02 - 2 cotyledons and 2 expanded leaves (Boyce *et al.*, 2001). At this stage, the plants were subjected to the assays described below.

#### **3.3 - Hydroponic system for *Arabidopsis* seedlings**

To establish a hydroponic system of growth, tip boxes of 200  $\mu\text{L}$ , reagents for culture medium (MS and MES), scotch tape, autoclaved distilled water and plastic cake boxes were used. The complete protocol will be presented in details at the results session.

#### **3.4 - Inhibition of the Target of Rapamycin (TOR) by AZD-8055**

The AZD-8055 was diluted in dimethylsulfoxide (DMSO) to a final concentration of 2  $\mu\text{M}$  per box and subsequently applied at the bottom of the boxes

where the roots are immersed. As control, DMSO in a concentration of 0.05% (v/v) was used. When plants reached the stage 1.02, a fresh liquid media containing AZD or DMSO was replaced into the hydroponic containers either at the end of day or at the end of night. Five pools of 35 seedlings each were collected per time point, immediately frozen in liquid nitrogen and stored at -80°C. To unravel the role of TOR in starch metabolism, harvest was performed in the following time-points: every 6 hours, 2 hours up to 12 or 24 hours as stated at the results section.

### **3.5 - Qualitative determination of starch content by lugol iodine**

Lugol iodine has been used to qualitatively monitor the content of starch in plants treated with 2  $\mu$ M AZD-8055 or 0.05% (v/v) DMSO. To this aim, seedlings were immersed in 80% (v/v) ethanol for 5 minutes at 95°C for pigment extraction and diafanization of the leaves after harvest according to the methodology of Lunn and Furbank (1997). Afterwards, samples were washed with distilled water and stained with lugol solution (iodine and potassium iodide). Finally, leaves were once again washed with distilled water and photographed in stereomicroscope Discovery V20, using the program Axio Vision 4.8, and the objective lens 0.63X, approximated 20X and magnitude 7.5X for comparison of the starch accumulation pattern from the color intensity between AZD-8055 and DMSO treated plants.

### **3.6 - Quantification of starch by enzymatic assay**

Frozen samples were ground to a fine powder in liquid nitrogen and aliquots of about 20 mg were prepared. The quantification of starch content was performed using the protocol described by Hendriks *et al.* (2003). Soluble sugars were extracted with 250  $\mu$ L of 80% (v/v) ethanol at 80°C for 20 minutes. Subsequently, samples were centrifuged at 20,000 *g* and the supernatants removed. This procedure was repeated three times. In order to destabilize the structure of the granules of starch and facilitate the action of starch degrading enzymes, 400  $\mu$ L of 0.1 M NaOH were added to the resulting pellet and incubated at 95°C for 30 minutes. After cooling at room temperature (RT), the extracts were neutralized with 0.5 M HCl containing 0.1 M acetate NaOH pH 4.9 (final pH around 6). Afterwards, 40  $\mu$ L of each extract were digested with amyloglucosidase (0.17U/well) and  $\alpha$ -amylase (0.24U/well) in 50 mM acetate-NaOH (pH 4.9) overnight at 37°C. After centrifugation at 4,000 *g* for 2 minutes at RT, aliquots of 40  $\mu$ L of the supernatant were transferred to another microplate and 160  $\mu$ L of

glucose quantification solution was added (100 mM HEPES/KOH, pH 7.0), 3 mM  $\text{MgCl}_2$ , 2.5 mM ATP and 1 mM  $\text{NADP}^+$ .

Determination of glucose released by the enzymatic digestion of starch was determined spectrophotometrically at 340 nm coupling the reduction of  $\text{NADP}^+$  to NADPH in a microplate reader (Stitt *et al.*, 1989). The amount of glucose was calculated from comparison with a calibration curve (0 – 20 – 40 – 80 nmols of glucose). Absorbance at 340 nm was monitored for about 45 minutes. For each sample, it was considered the absorbance average of two technical replicates and reactions that were completed when the absorbance did not changed more than 0.03 nm (tolerance) from the previous measurement cycle. Data were normalized according to plate internal concentration standards, volume and sample weight. Starch content was modelled with the help of linear model function, adding time, drug and the interaction effects sequentially to the statistical model. For each effect addition, the resulting model was compared with the previous one with the help of anova function. It was chosen the model with best fit to the observed data. All statistical analysis was performed in R software version 3.2.0 (R Core Team, 2015).

### **3.7 - Quantification of primary metabolites**

Primary metabolites were extracted from approximately 20 mg of fresh weight following the methodology described by Giavalisco *et al.* (2011). This extraction allows the separation between polar and non-polar phases. Aliquots of 150  $\mu\text{L}$  of the polar phase were dried in a vacuum concentrator and derivatized for analysis by gas chromatography (7890N, Agilent) coupled to Time-of-flight (TOF) mass spectrometry (Pegasus HT, Leco) (Lisec *et al.*, 2006). Acquisition parameters of chromatograms were identical to those described for Weckwerth *et al.* (2008). Chromatograms were exported from Leco Chroma TOF (version 3.25) program to R 2.12.2 program. Detection of the peaks, the retention times alignment and searching in libraries were made by using the package Target Search of the Bioconductor (Cuadros- Inostroza *et al.*, 2009).

Metabolites have been quantified for peak intensity of a selected mass, which was normalized for the fresh weight of the samples and total ion count (TIC), and a logarithmic transformed on base 2. A t-test was used to determine significantly differences in metabolite levels between treatments.

### 3.8 – Gene expression analysis

The relative gene expression analysis was performed in order to monitor marker genes of TOR - L25a, L19, 5.8S-I, 5.8S-II, CNP10a, EFTua, L14, ATG9, ATG18 (Tatematsu *et al.*, 2005), TOR (Caldana *et al.*, 2013) and AGPase subunits (Mugford *et al.*, 2014). Primer sequences are in **Table 1**, supplemental material. Total RNA extraction, cDNA synthesis and analysis by real time PCR were carried out as described by Caldana *et al.* (2007) and Czechowski *et al.* (2005). Total RNA has been extracted from a pool of 3 biological replicates (35 plants/replicate) with RNeasy Plant Mini Kit (Qiagen) according to manufacturer's instructions. Contamination with genomic DNA has been removed through treatment with Turbo DNA-free DNase (Ambion). RNA integrity was assessed by agarose gel electrophoresis and Bioanalyzer prior to cDNA synthesis.

The relative expression analysis was analyzed in 384 well optical plates through the system “ViiATM7 Real-Time PCR system” (Applied Biosystems), using SYBR green PCR master mix (Applied Biosystems) – (Hold stage 50°C 2 min, 95°C 10 min; PCR stage 95°C 15 sec, 60°C 1 min for 40 times; Melt curve stage 95°C 15 sec, 60°C 1 min, 95°C 15 sec).. Relative quantification was done with 3 biological replicates using ubiquitin and PDF2 as housekeeping genes (Czechowski *et al.*, 2005). The relative expression was calculated by subtracting the CT value of the gene of interest from the geometric mean of CT values of the reference genes, resulting in  $\Delta CT$ . A t-test was performed to verify if there were significantly differences in relative gene expression between treatments.

### 3.9 - Maximal catalytic activity of ADP-glucose pyrophosphorylase (AGPase)

Soluble proteins were extracted from 20 mg of leaves in buffer containing 10% (v/v) glycerol, 0.25% serum bovine albumin (w/v), 1% (v/v) Triton – X100, 50 mM HEPES/KOH pH 7.5, 10 mM MgCl<sub>2</sub>, 1mM EDTA, 1 mM EGTA, 1mM benzamidine, 1 mM aminocaproic acid, 1mM methyl sulfonyl fluoride, 10 mM leupeptin and 0.5 mM dithiothreitol (Gibon *et al.*, 2004).

ADP-glucose pyrophosphorylase was assayed in the reverse direction by measuring the PPi-dependent production of ATP from ADP-glucose, in optimized conditions of substrates, cofactors, activators and pH (Gibon *et al.*, 2004). Extracts and standards (ATP ranging from 0 to 1 nmol) were prepared in the extraction buffer and incubated in a medium containing 50 mM Hepes/KOH, pH 7.5, 5 mM MgCl<sub>2</sub>, 1 U.mL<sup>-1</sup>

glycerokinase (obtained by heterologous expression of the glycerokinase-encoding *GUT1* gene from *Pichia farinosa* according to Gibon *et al.*, 2009), 0 (blank) or 1 mM (maximal activity) ADP-glucose, 5 mM 3-phosphoglycerate, 1.5 mM sodium fluoride, and 120 mM glycerol. The reaction was started by the addition of PPi to a final concentration of 2 mM. The reaction was stopped with 20  $\mu$ L of 0.5 M HCl. After neutralization with 20  $\mu$ L of 0.5 M NaOH, glycerol-3-P was measured as described in Gibon *et al.* (2002), in the presence of 1.8 U.mL<sup>-1</sup> glycerol-3-P oxidase, 0.7 U.mL<sup>-1</sup> glycerol-3-P dehydrogenase, 1 mM NADH, 1.5 mM MgCl<sub>2</sub>, and 100 mM Tricine/KOH, pH 8.0. The absorbance was read at 340 nm until the rates were stabilized and rates of reactions were calculated as the change in the absorbance (OD min<sup>-1</sup>). A t-test was used to determine significant differences in enzyme activity between treatments.

### **3.10 - Immunoblotting analysis of ADP-glucose pyrophosphorylase (AGPase)**

Prior to enzyme extraction, 30 mg of fresh weight were pre-treated with 10 volumes of trichloroacetic acid 16% in diethyleter (fresh weight/v) to avoid the conversion from dimeric to monomeric form and incubated at -20°C overnight. Subsequently, samples were centrifuged at 4°C for 5 minutes at 20,000g and washed 3 times with 800  $\mu$ L of cold acetone (Hendriks *et al.*, 2003). After centrifugation at 20,000g, pellets were dried in speed-vacuum for 30-45 minutes. Ten volumes of sample buffer (Laemmli) (fresh weight/v) were added. A non-reducing SDS-polyacrylamide gel (10%) was prepared and 25  $\mu$ L of the extracts were loaded. The running buffer was composed of 25 mM Tris, 200 mM glycine and 0.1% SDS. Electrophoresis was performed for 1 h at 200 V. AGPase was detected using a primary rabbit antibody raised against the small subunit from *A. thaliana* (AS111739 Agrisera, 1:3000 in blocking buffer), followed by anti-rabbit IgG horse radish peroxidase conjugated (AS09602 Agrisera, 1:15000 in blocking buffer). Immunoreactive proteins were detected by incubation of the immunoblots with luminol/enhancer solution and peroxide solution (1:1) (Cyanagen), using an Image Quant LAS 500 (GE Healthcare) CCD imager.

### **3.11 - Measurement of reduced and oxidized glutathione**

Samples were extracted and measured exactly as described by Queval and Noctor (2007). Aliquots (50 mg) were extracted with 0.5 ml of 0.2 N HCl, well mixed and centrifuged at 16,000g for 10 minutes at 4°C. The samples were neutralized with



20  $\mu$ l of 0.2 M  $\text{NaH}_2\text{PO}_4$  (pH 5.6), followed by the stepwise addition of 0.2 M NaOH, and the final pH was between 5 and 6.

Glutathione determination relies on the glutathione reductase-dependent reduction of 5,5'-dithiobis(2-nitro-benzoic acid) (DTNB, Ellman's reagent), monitored at 412 nm. Without pre-treatment of extracts, the method measures "total glutathione", reduced glutathione (GSH) plus oxidized glutathione GSSG. Specific measurement of GSSG was achieved by pre-treatment of extract aliquots with 2-vinylpyridine (VPD), as described by Griffith (1980).

To measure total glutathione, triplicate aliquots of 10  $\mu$ l neutralized extract were added to plate wells containing 0.1 ml of 0.2 M  $\text{NaH}_2\text{PO}_4$  (pH 7.5), 10 mM EDTA, 10  $\mu$ l of 10 mM NADPH, 10  $\mu$ l of 12 mM DTNB, and 60  $\mu$ l of water. The reaction was started by the addition of 0.187 U glutathione reductase (GR). The increase in  $A_{412}$  was monitored for min. Standards (0 to 1 nmol GSH) were run concurrently in the same plates as triplicate. Rates were calculated over the 5 minutes and in all cases were corrected for GSH-independent reduction of DTNB by subtraction of the mean value of triplicate blank assays (0 GSH). GSSG was measured by the same principle after incubation of 0.2 ml neutralized extract with 1  $\mu$ l VPD for 30 minutes at RT to complex GSH. To remove excess VPD, the derivatized solution was centrifuged once (10 minutes at 10570 r.p.m. and triplicate 20- $\mu$ l aliquots of the final supernatant were assayed as described above. GSSG standards (0 to 80 pmol) run concurrently were subjected to the same VPD derivatization as the extracts. Rates were calculated as for total glutathione and corrected by subtraction of the blank. A t-test was used to determine significant differences in glutathione levels between treatments.

## 4 - Results and Discussion

### 4.1 - Establishment of a hydroponic growth system to investigate the role of TOR on *Arabidopsis* seedlings

The use of chemical inhibitors has been proved to be a useful tool to dissect TOR function in plants. These new TOR inhibitors, including AZD-8055, are ATP competitive because they target the ATP-binding site of the kinase domain (Dowling *et al.*, 2010). However, its application must be regarded with caution as a balance between toxicity and efficacy must be achieved to prevent the use of high concentrations of inhibitors, which could trigger secondary effects on plants. A previous work from our research group aimed to evaluate the best AZD-8055 dose to efficiently inhibit the TOR complex without causing severe toxicity. The results from this work suggested that a concentration of 2  $\mu$ M AZD-8055 was required to inhibit 50% of growth (IC<sub>50</sub>) after 3 days and therefore this concentration was chosen to be used in the present work (data not shown).

Generally, assays using chemical inhibitors are performed in liquid medium to ensure the contact between plants and solution. To characterize the dynamics of starch synthesis and degradation in TOR-inhibited plants, seeds of *A. thaliana* Col-0 were grown in solid medium until they reached stage 1.02 (Boyce *et al.*, 2001) (approximately 11 days), and then transferred to Erlenmeyer's containing liquid medium with the chemical inhibitor or DMSO (as control). Samples were harvested every 4 hours for a period of 24 hours in an experiment starting at the end of day. It has been shown in the literature that the starch content in *A. thaliana* increases linearly during the day and diminishes linearly along the night in a diel-cycle of 12 h light/12 h dark (**Figure 4.1 A**) (Gibon *et al.*, 2004). In our assay, the pattern of starch content even for the control (DMSO) did not follow the pattern shown in the literature. In addition, the levels of this polymer were very similar in seedlings treated with AZD-8055 and DMSO (**Figure 4.1 B**). Furthermore, this result disagree with the findings that TOR-silenced plants present a starch excess phenotype in comparison to control (Moreau *et al.*, 2012; Caldana *et al.*, 2013; Dobrenel *et al.*, 2013).

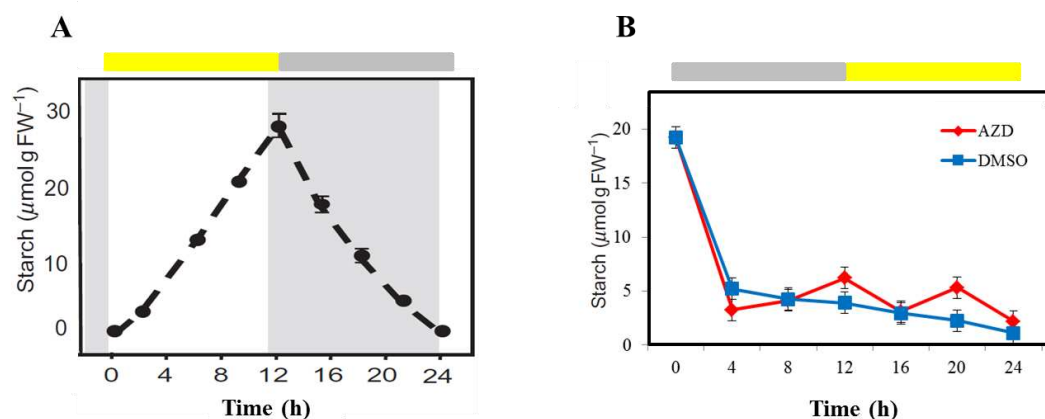


**Figure 4.1 - Pattern of starch content in a diel-cycle shown in the literature and in our assay in seedlings of *Arabidopsis thaliana* treated with AZD-8055 (TOR-inhibitor) and DMSO (Control).**

(A) Pattern of starch content in a diel cycle of 12 h light/12 h dark presented in the literature (Gibon *et al*, 2004); (B) Pattern of starch content in our assay. AZD-8055 (red line) and DMSO (blue line) were administrated in 11 day-old plants at the end of day and samples were harvested every 4 h during the night (grey bar) or (yellow bar) for 24 h. Values shown are mean  $\pm$  SE of 5 biological replicates containing 35 plants each.

During seedlings shift from solid to liquid medium, mechanic manipulation was imposed. Although the seedlings were transferred carefully, we cannot totally exclude mechanical damage due to the number of seedlings handled, what might affect the starch content. It has been shown that plants very often accumulate starch due to impaired growth in stressed conditions and that the content of this polymer is negatively correlated with growth (Sulpice *et al.*, 2009). Since starch metabolism is sensitive to stress conditions, we hypothesized that the lack of a typical starch profile pattern in a diel cycle could be attributed to the growth system.

To evaluate if seedlings were stressed after transference, starch content was qualitatively measured after transferring the seedlings from solid to liquid media using iodine-lugol method (Lunn and Furbank, 1997). Lugol, a compound formed by elemental and potassium iodide, is able to complex with amylose and amylopectin molecules belonging to the structure of starch, resulting a blue and red color, respectively. Since *A. thaliana* plants consume starch in almost its totality during the night, it is expected a low content of this polymer at the beginning of day in unstressed plants (Gibon *et al.*, 2004). The high starch staining at the beginning of day in seedlings of *Arabidopsis* after transference confirmed that the normal kinetic of starch was impacted as a consequence of manipulation and transference between medium (Supplementary Figure S1 A).

To overcome the stress caused by transferring the seedlings, a hydroponic system was developed using 200  $\mu\text{L}$  tip boxes to facilitate the drug administration, avoid

mechanical injuries and allow application of any chemical treatment in large scale. **Figure 4.2** illustrates the workflow of the hydroponic system. Tip boxes were autoclaved and the top of the boxes inverted onto adhesive tape (**Figure 4.2 A**) where 200  $\mu$ L of solid medium containing  $\frac{1}{2}$  MS + MES + Agarose 0.8% were added (**Figure 4.2 B**). Subsequently, 350 ml of liquid culture medium containing  $\frac{1}{2}$  MS + MES were placed at the bottom of the box (**Figure 4.2 C**). After medium solidification, adhesive tapes were removed and surfaced-sterilized *A. thaliana* seeds were placed at the top of the tip box (**Figure 4.2 D and E**). The top and bottom of the tip box were assembled inside plastic packing boxes to maintain a high humidity (**Figure 4.2 F**). Plastic packing boxes were placed into a growth chamber with 75% of humidity, 150  $\mu$ mol m<sup>-2</sup> s<sup>-1</sup> of irradiance, and equinoctial conditions (12 h light/21°C, 12 h dark/19°C). Plant growth was monitored until the stage 1.02 (Boyce *et al.*, 2001) with 2 cotyledons and 2 expanded leaves (**Figure 4.2 G**).

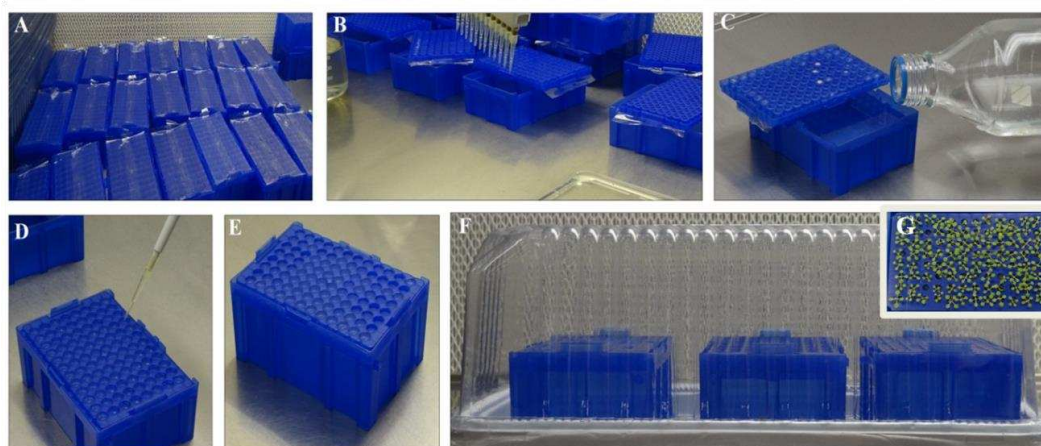


**Figure 4.2 - Workflow for a hydroponic system to grow *Arabidopsis thaliana* seedlings.** (A) First, adhesive tape was attached to the upper tip boxes and (B) solid  $\frac{1}{2}$  MS medium containing MES was added. Then, (C) liquid medium containing  $\frac{1}{2}$  MS + MES was added to the bottom of the box and (D, E) seeds were placed in the orifices of the upper part of the boxes. (F) The boxes were placed in plastic packing boxes to maintain a high humidity. (G) Seedlings after growing for 11 days-old in hydroponic system.

In this system, germination of seeds and seedling growth rates followed the same developmental pattern as observed in Petri dishes. To evaluate if plant growth in hydroponic system would affect the starch content, a fresh medium containing AZD-8055 or DMSO was replaced on the end of the dark period when seedlings reached 11 days after seeding (DAS). Starch content was monitored qualitatively (**Supplementary Figure S1 B**) and quantitatively (**Figure 4.3**), at the time points 0, 12 and 24 hours after treatment. As shown in **Supplementary Figure S1 B**, starch content followed the same

pattern as observed **Figure 4.1 A** regardless of the treatment, indicating that seedlings seem to be unstressed when they were transferred to a fresh medium in the hydroponic system. Likewise, starch quantification in a diel-cycle showed a similar linear pattern of synthesis and degradation as already observed in previous works (**Figure 4.3**).

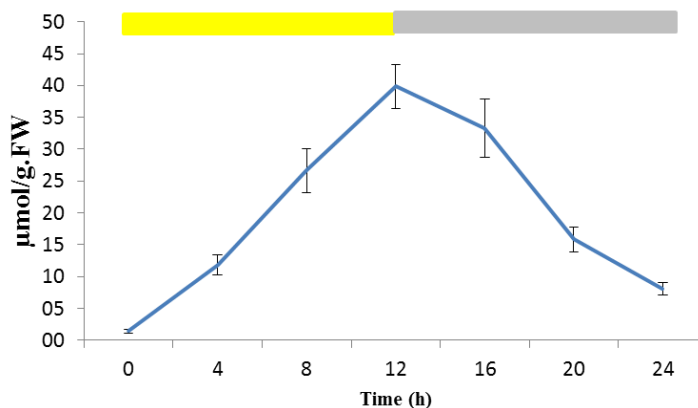


**Figure 4.3 - Starch content from seedlings grown in our hydroponic system.**

Samples of 11 days-old plants were harvested every 4h during the day (yellow bar) and every 4h during the night (grey bar) for 24h. Values shown are mean  $\pm$  SE of 5 biological replicates containing 35 plants each.

Next, the uptake of the AZD-8055 by the seedlings in the hydroponic system was monitored using a UPLC-MS/MS analysis. The results revealed that AZD-8055 is already translocated into the shoots after 1 hour of treatment (data not shown). This data is in agreement with the observation that 30 minutes after AZD-8055 treatment is able to trigger autophagy in leaves (Meyer *et al.*, personal communication).

The identification of the exact moment in which TORC is molecularly inhibited by AZD-8055 is crucial to find out its direct targets. In most eukaryotic species, the major readout of TOR activity is the phosphorylation of the S6K at the protein level. However, the levels of this protein are very low in plants, precluding the detection with antibodies. Attempts to the identification of other direct targets revealed a possible role of TOR in regulating the transcription of genes encoding for components of ribosome biogenesis (Hay and Sonenberg, 2004; Ren *et al.*, 2011). Therefore, the expression of selected genes involved in ribosome biogenesis (ARP, CPN10A, EFTu, L14, L19, L35) was tracked using qRT-PCR (Tatematsu *et al.*, 2005). The expression profile of those genes was monitored at 15, 30, 60, 120, 240 and 360 minutes after treatment (AZD-8055 or DMSO). As shown in **Figure 4.4**, the relative abundance of transcripts of all genes tested was lower in TOR-inhibited plants after 240 minutes of treatment when compared with the control. These results provided further evidence that the inhibition of TOR complex occurred within the first 4 hours of treatment.

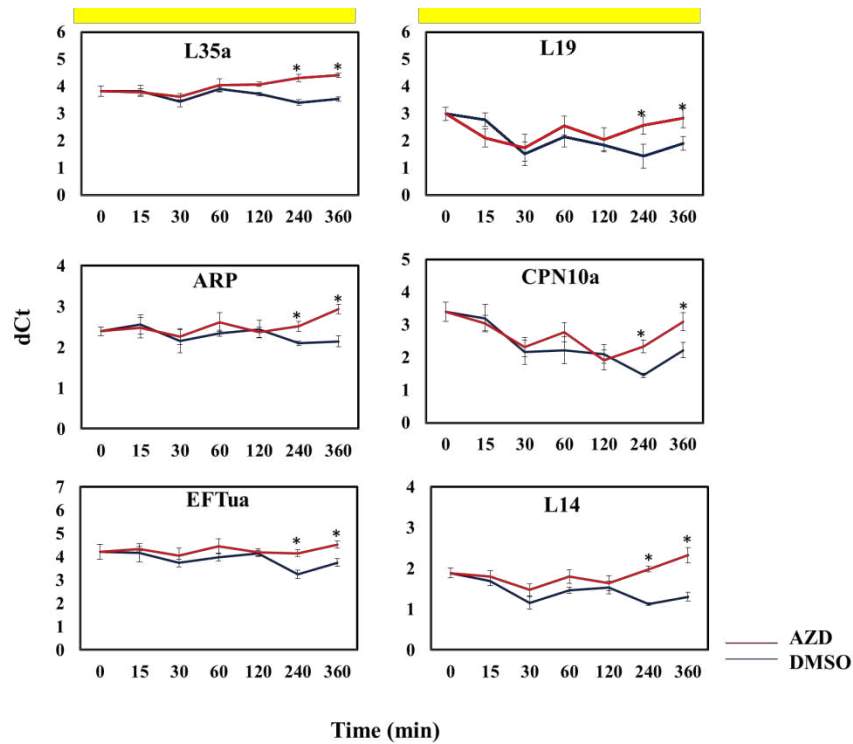


**Figure 4.4 - Gene expression analysis of ribosome biogenesis-related genes in AZD-8055 and DMSO treated plants.**

Gene expression analysis of ARP, CPN10A, EFTu, L14, L19 and L35a was determined by qRT-PCR from samples in which AZD or DMSO was applied at the end of night. Relative abundance of transcripts was calculated by subtracting the  $C_T$  of the targets for the geometric mean  $C_T$  of two housekeeping genes (PDF2 and UBQ). Values shown are mean  $\pm$  SE of 5 biological replicates containing 35 plants each. Red lines: AZD-8055-treated plants; Blue lines: DMSO-treated plants; Yellow bar (light); Significant differences between the AZD-8055 and DMSO treated plants, using Student's t-test, are indicated by asterisks \* ( $P < 0.05$ ).

## 4.2 - TOR-inhibited plants have increased starch synthesis

As autotrophic organisms, plants are particularly attuned to the diurnal light-dark cycle due to their dependence on sunlight for photosynthesis, and their circadian clock helps to integrate processes such as gene expression, metabolite and enzyme levels, and growth to the diurnal rhythm in C and energy supplies (Gibon *et al.*, 2006; Harmer, 2009; Graf *et al.*, 2010). Prior to starch analysis, TOR gene expression pattern in a diel-cycle was evaluated. This analysis could provide a hint if TOR is regulated by a diel-cycle. As shown in **Figure 4.5**, TOR-gene expression tends to increase during the day and decreases during the night. Preliminary results from our group indicated that the protein level of TOR follows the same dynamics as the transcripts (data not shown). During the day, in conditions where photosynthesis is occurring, several anabolic processes (macromolecules biogenesis, translation, etc) take place as a consequence of available energy. Since TOR is responsible to integrate energy status promoting growth through several biological processes, the result presented in **Figure 4.5** is in accordance

with the pattern of energy production during the day and its sensing by signaling proteins, this being represented by the increase in TOR-expression along the day.

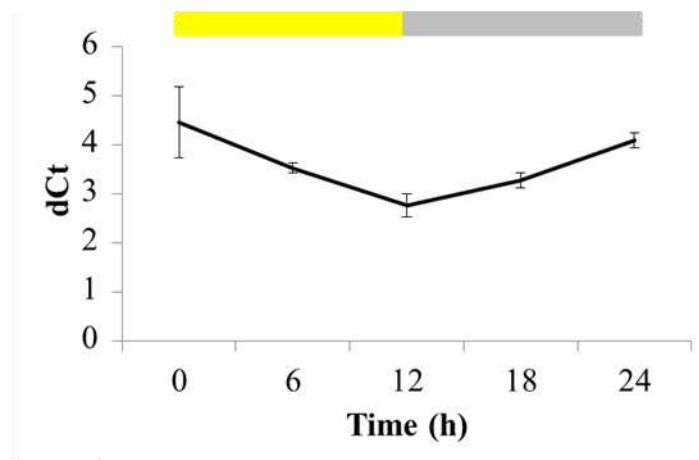


**Figure 4.5 - Pattern of TOR-gene expression in a diel-cycle.**

Gene expression analysis of TOR gene was determined by qRT-PCR from samples harvested every 6 hours during 24h. Relative abundance of transcripts was calculated by subtracting the  $C_T$  of the targets for the geometric mean  $C_T$  of two housekeeping genes (PDF2 and UBQ). Values shown are mean  $\pm$  SE of 5 biological replicates containing 26 plants each. Yellow bar (light); grey bar (dark).

Previous works have shown that plants in which genes encoding for TOR complex are silenced display a starch excess phenotype (Moreau *et al.*, 2012; Caldana *et al.*, 2013; Dobrenel *et al.*, 2013). However it remains to be elucidated whether this phenotype is triggered by an increase in synthesis, impaired degradation or both. Furthermore, starch-related phenotypes are very common to occur in mutants with impaired growth, as it is the case of the ones from the TOR complex. Therefore, a kinetic analysis of starch upon AZD-8055 treatment would also allow identifying if the starch metabolism is a direct target of the TOR complex. To address these questions, two assays were performed: AZD-8055 and DMSO (control) were applied at the end of night (EN) or at the end of day (ED) and in both cases samples were harvested every 6 hours during 24 hours and this polymer was enzymatically quantified.

To evaluate the differences in rates of starch synthesis and degradation, a linear regression was performed to verify the effect of drug application over time. Visually, differences between treatments can be observed by the angle and distance formed between the red (AZD-8055) and blue (DMSO) lines. The bigger is the distance and the angle between lines, the most prominent is the difference between treatments (**Figure 4.6**).

Independently from the time of drug administration (ED or EN) the rates of starch synthesis were significantly higher in plants treated with AZD-8055 than in non-



treated plants (**Figure 4.6 A and B**). In contrast, there was no effect of drug application in the rate of starch degradation during the first 12 hours of darkness (**Figure 4.6 B**). However, as shown in **Figure 4.6 A**, the difference in the rate of starch degradation was only observed after periods superior to 12 hours of treatment, indicating that changes in the rate of starch degradation might be a secondary effect of TOR inhibition. All together, these results suggested that the starch excess phenotype observed in TOR-inhibited plants was due to increase in starch synthesis rate.

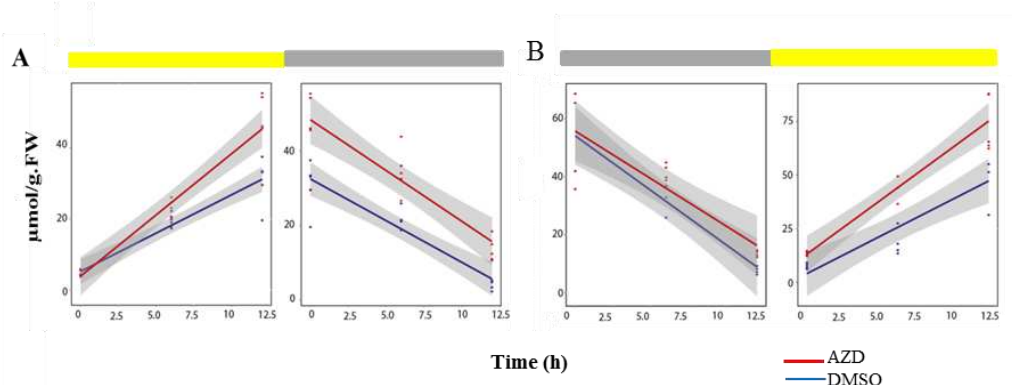


**Figure 4.6 - Rates of starch synthesis and degradation of seedlings treated with AZD-8055 and DMSO (control), sampled every 6 hours for 24 hours.**

The effect of 2  $\mu$ M AZD-8055 treatment on starch metabolism was assessed by linear regression analysis when the TOR inhibitor was applied at the end of night (**A**) or end of day (**B**). 11 day-old plants were harvested every 6 h during the day (yellow bar) and every 6 h during the night (grey bar) for 24 h, in two independent experiments. Values shown are mean rates of starch synthesis and degradation of 5 biological replicates containing 26 plants each. Student T-test has been performed at the 0.05 level of significance, Red line (AZD), Blue line (DMSO).

Since the starch excess phenotype was observed after 6 hours of AZD-8055 treatment, we next evaluated the effect of TOR inhibition on starch synthesis in a shorter time-frame (every 2 hours), following the same procedures described above. Linear regression confirmed our previous results that TOR does not directly impact the starch degradation (**Figure 4.7 B**). In contrast, changes in starch synthesis were already detected after 4 hours of TOR inhibition, presenting an average increase of 20-30% in their starch content at the ED when compared to control (**Figure 4.7 A**). These data confirmed a possible role of TOR regulating starch synthesis.



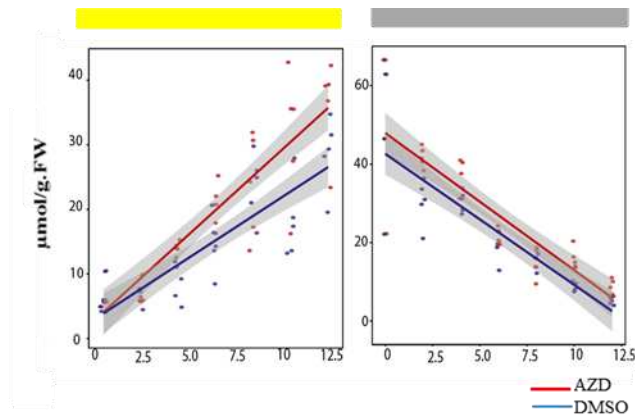


**Figure 4.7 - Rates of starch synthesis and degradation of seedlings treated with AZD-8055 and DMSO (control) sampled every 2 hours for 12 hours.**

The effect of 2  $\mu$ M AZD-8055 treatment on starch metabolism was assessed by linear regression analysis when the TOR inhibitor was applied at the end of night (A) or end of day (B). 11 day-old plants were harvested every 2 h during the day (yellow bar) and the night (grey bar) for 12 hours, in two independent experiments. Values shown are mean rates of starch synthesis and degradation of 5 biological replicates containing 26 plants each. Student T-test has been performed at the 0.05 level of significance, Red line (AZD), Blue line (DMSO).

### 4.3 - Repression of TOR complex impacts metabolites related to starch metabolism

Starch metabolism is very complex, involving many steps of regulation, compartmentalization, and it competes with other pathways such as sucrose. In order to assess the impact of TOR inhibition on other pathways related to starch synthesis, the sucrose, fructose, glucose, mannose, maltose and orthophosphate (Pi) were quantified by GC-TOF-MS (Figure 4.8).

Sucrose and starch are the primary products of photosynthesis, and their syntheses compete to each other during the day. Sucrose is the major sugar transported throughout the plant body and has a crucial role in cellular respiration and/or in other metabolic processes, can be transported to sink organs or stored in the vacuole. The excess of sucrose regulates negatively its synthesis and positively the synthesis of starch in the chloroplast (Sulpice *et al.*, 2009). The Figure 4.8 A1 and A2 show the decrease of sucrose in TOR-inhibited plants over time and this is in accordance with the increment in starch levels observed at the same time points. In normal conditions, the amount of starch begins to increase only when an excess of sucrose is produced (Ruan, 2014). Our results are in agreement with the levels described in the literature for both sucrose and starch, and pointed out the possibility of an influence of TOR on sucrose metabolism and not directly on starch metabolism.

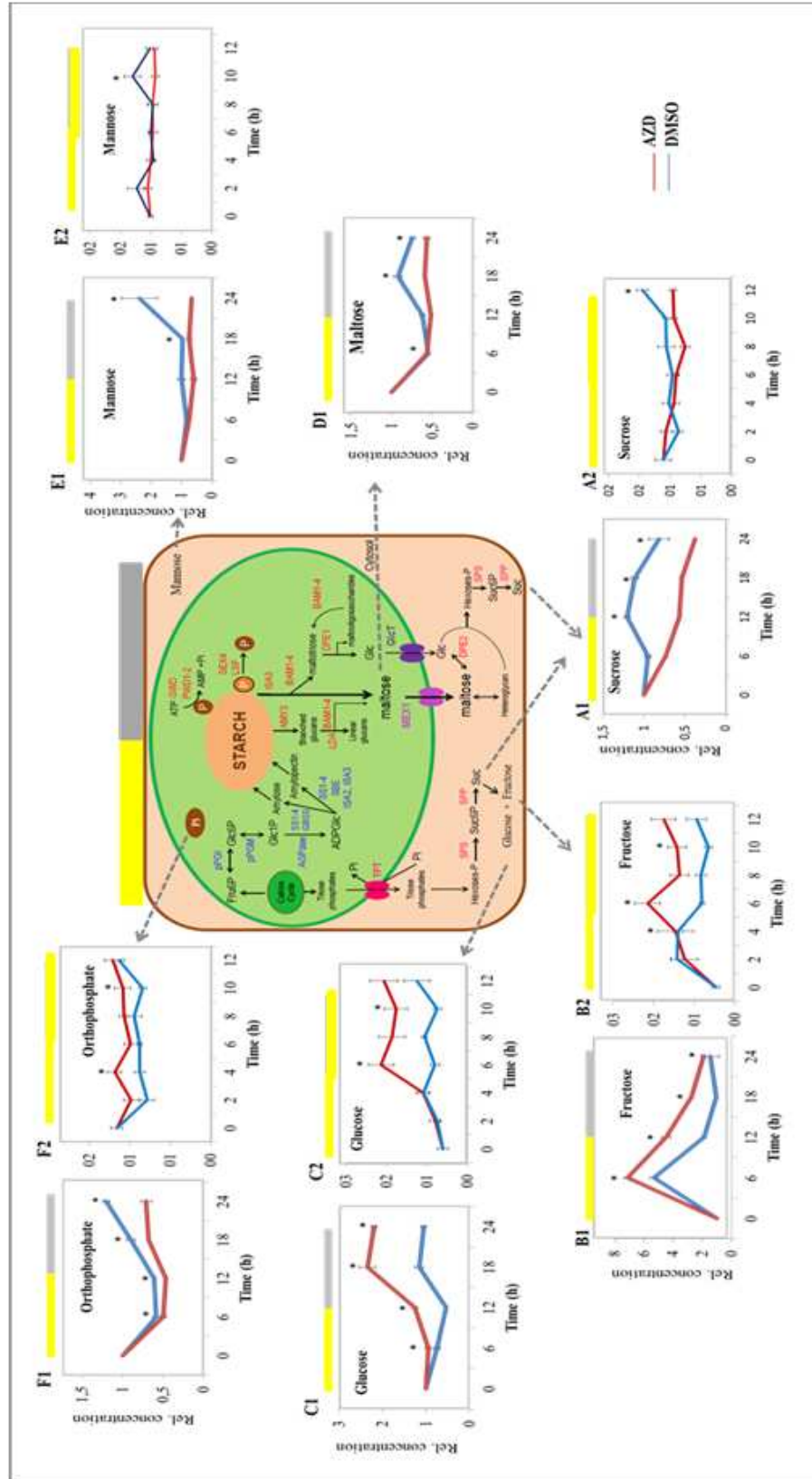


**Figure 4.8-Levels of metabolites related to starch metabolism quantified in plants treated with AZD-8055 and DMSO (control) collected every 6 h for 24h and every 2h for 12h starting at the end of night.**

The content of (A1, A2) Sucrose, (B1, B2) Fructose, (C1, C2) Glucose, (D1) Maltose, (E1, E2) Mannose and (F1, F2) Orthophosphate were determined using GS-MS. Samples of 11 days-old plants were harvested every 2h and 6h during the day (yellow bar) and every 6h during the night (green bar) for 12h and 24h in two independent experiments, both starting at the end of night. The results are the mean  $\pm$  SE of metabolite relative abundance- (26 plants/5 biological replicates). Significant differences between the AZD-8055 and DMSO treated plants, using Student's t-test, are indicated by asterisks \* ( $P < 0.05$ ).

The regulation of photosynthesis, starch and sucrose metabolism occurs in various ways, involving various sugars and interacting pathways (Goldschmidt and Huber, 1992). Glucose and fructose are products of sucrose breakdown. Sucrose is not the only source for the formation of these sugars, but it has a great importance to maintain their homeostatic levels. These two sugars participate in a wide range of metabolic processes, mainly in cellular respiration. The levels of glucose and fructose may regulate photosynthesis and consequently influence starch metabolism. Since the amount of sucrose decreased in TOR-inhibited plants, an augmentation of fructose and glucose was expected as it could be confirmed in **Figures 4.8 B1, B2, C1 and C2**, respectively. Interestingly and in accordance with previous works (Deprost *et al.*, 2007; Caldana *et al.*, 2013), the content of fructose was shown to be always higher in TOR-inhibited plants in the first 2 hours of TOR inhibition. The same pattern was not observed for glucose, which levels started to raise only after 6 hours of AZD-8055 treatment (**Figure 4.8 C2**). These data open a new perspective in the study of the regulation of TOR pathway, but it remains to be elucidated whether the total amount of glucose and fructose is formed only as a consequence of sucrose breakdown or due to other interacting pathways as a consequence, for example, of impaired respiration.

Maltose is the main sugar released from the chloroplast after starch breakdown and is crucial in maintaining plant metabolism during the night (Weise *et al.*, 2004). Its content was greater in AZD-treated plants during the day compared with the control (**Figure 4.8 D**). However, during the night, its levels tended to be lower in AZD-treated plants most probably due to impaired degradation. Interestingly, the maltose pattern does not follow the expected pattern of starch content during the day. However, the lower levels of maltose content in the TOR inhibited plants at the EN might also indicate a reduction in starch degradation, probably as a secondary effect of TOR inhibition.

In light conditions, the synthesis of starch takes place and one of the most important regulatory enzyme responsible for this process is AGPase (Kavakli *et al.*, 2002). This enzyme is located inside the chloroplast and some metabolites are able to regulate its activity. The high ratio of 3-PGA/Pi controls positively the activity of AGPase and high amounts of Pi impair its activity. Levels of Pi inside and outside the chloroplast are balanced to promote starch and sucrose synthesis (Edwards and Walker, 1983). There are various reactions that use Pi and can reduce its content. For example,

mannose is a known sugar to be involved in sequestering free-Pi in the cytosol and promoting synthesis of starch through the allosteric inhibition of AGPase activity (Herold *et al.*, 1976; Heldt *et al.*, 1977; Hnilo and Okita, 1989). In TOR-inhibited plants, the levels of mannose (**Figure 4.8 E1 and E2**) tended to be lower after 10 hours of treatment when compared to the control plants, suggesting a possible reaction of this metabolite with the cytoplasmic Pi forming mannose-6-phosphate. Similarly, the levels of Pi were decreased after 4 hours of TOR inhibition (**Figure 4.8 F1 and F2**). Although the pattern of mannose and Pi followed a similar dynamic after TOR inhibition, the kinetics of their response might suggest that those metabolite changes are a secondary effect of AZD treatment. To corroborate this hypothesis, it would be important to determine the levels of other sugar phosphates such as mannose-6-phosphate to verify if short changes in these sugars are observed and link it to the starch excess phenotype presented in TOR-inhibited plants.

#### **4.4 – Analyses of gene expression, catalytic activity and immunoblotting of ADP-glucose pyrophosphorylase (AGPase)**

One of the first regulatory steps in starch synthesis and also regulated by the levels of mannose and Pi involves ADP-glucose pyrophosphorylase (AGPase). This heterotetrameric enzyme is subject to several levels of post-translational regulation (Morell *et al.*, 1987; Okita *et al.*, 1990). The content of sucrose in cytosol can regulate the flux into starch due to the allosteric properties of this enzyme. Similarly, high levels of triose-phosphates in the chloroplast result in high 3-phosphoglyceradehyde (3-PGA) levels, activating the AGPase. Conversely, high Pi levels inhibit AGPase activity (Geigenberger *et al.*, 2005; Mugford *et al.*, 2014).

The genome of *A. thaliana* has 4 genes encoding for the large subunits (APL1, APL2, APL3 and APL4) and only one encoding for the small subunit (APS1). Depending on the its assembled, AGPase can assume different catalytic activities (Mugford *et al.*, 2014). With the aim of determining if the inhibition of TOR led to changes in the expression of AGPase subunits, gene expression analysis was performed in samples collected every 6h for 24h. As shown in **Figure 4.9**, significantly differences in gene expression between treatments occurred only after 18h after drug treatment for the subunits APL3 and APL4. Whereas APL3 expression was increased, APL4 transcript level was decreased in TOR-inhibited plants compared with the control. Mugford *et al.*, (2014), showed that large subunits may be differentially expressed in

response to environmental stimuli. It has been widely reported that repression of TOR activity mimics a starvation response. Therefore, one could speculate that changes in the transcript levels of those two large subunits could be triggered as a secondary effect of the low energy/starvation-like phenotype of TOR inhibition.

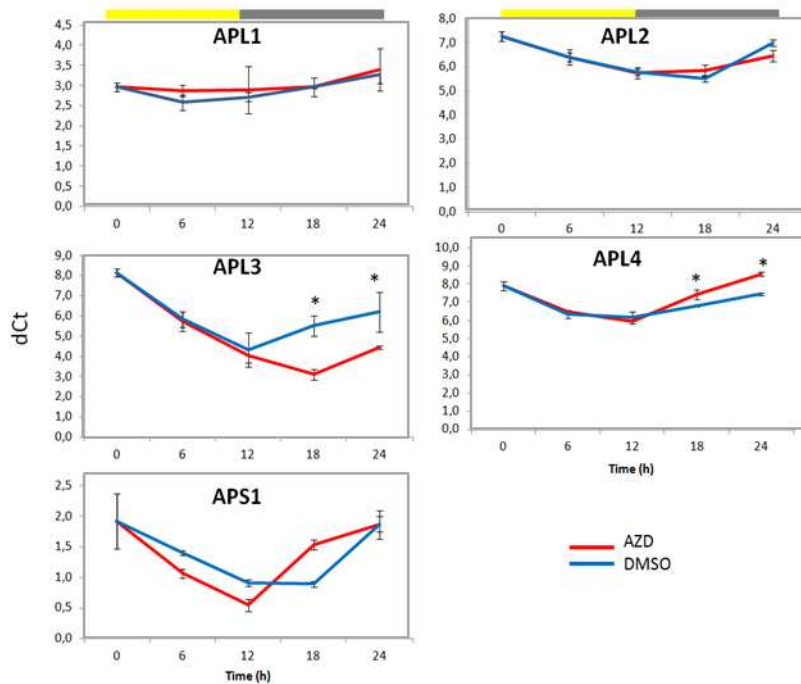


**Figure 4.9 - Gene expression analysis of AGPase subunits in AZD-treated plants and non-treated plants.** APL1, APL2, APL3 and APL4 represent large subunits and APS1 the small subunit of AGPase, respectively. Relative abundance of transcripts was calculated by subtracting the  $C_T$  of the subunits for the geometric mean  $C_T$  of two housekeeping genes (PDF2 and UBQ). The values are the mean  $\pm$  SE (35 plants/5 biological replicates). Red lines: AZD-8055-treated plants; Blue lines: DMSO-treated plants; Yellow bar (light); Grey bar (night). Significant differences between the AZD-8055 and DMSO treated plants, using Student's t-test, are indicated by asterisks \* ( $P < 0.05$ ).

Since the main goal of this work is to investigate whether TOR is involved in the direct regulation of starch synthesis, as next, a kinetics analysis of AGPase activity was determined by enzymatic assays, which access the maximum catalytic activity, an essential parameter to understand how enzymes operate in metabolic networks (Stitt and Gibon, 2014). Since the starch excess phenotype was detected 4h after AZD-8055 treatment, AGPase catalytic activity was first assessed 2h after AZD-8055 administration to investigate early regulation. **Figure 4.10** shows that AZD-treated plants presented significantly lower AGPase activity in the time points of 4 and 24 hours after treatment. Due to the starch excess phenotype presented in TOR-inhibited plants, we would expect a higher AGPase activity in these plants in case of TOR regulates the activity of this protein. Although TOR inhibition leads to the changes in

AGPase activity, these modifications are probably not responsible for the increase in starch synthesis.

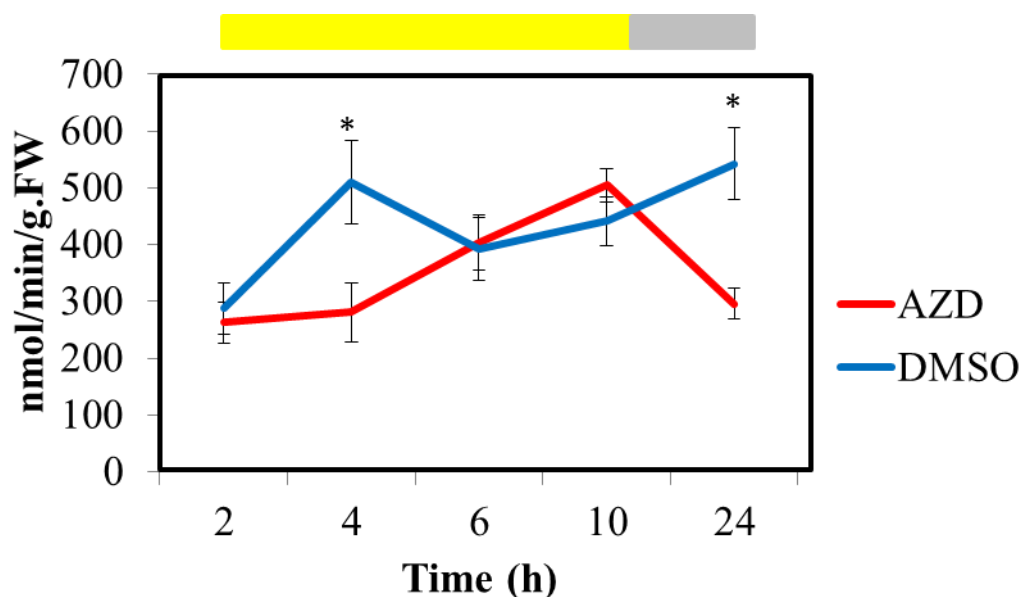


**Figure 4.10 - Catalytic activity of AGPase in AZD-treated plants and non-treated plants**

Catalytic activity of AGPase at the time points 2, 4, 6, 10h after treatment during the day (yellow bar) and night (grey bar). The results are the mean of AGPase activity - (26 plants/5 biological replicates). Significant differences between the AZD-8055 and DMSO treated plants, using Student's t-test, are indicated by asterisks \* ( $P < 0.05$ ).

Previous studies have shown that this protein is subject to redox regulation (Hendriks *et al.*, 2003). The regulatory enzyme is assembled in two small and two large subunits to compose the heterotetramer. The two small subunits have an intermolecular disulphide bridge linking the Cys81 residues (Hadrach *et al.*, 2012). During the light, this enzyme is active in its monomeric form (50 kDa), whereas, during the night or in dark conditions, AGPase is inactivated by the intermolecular disulphide bridge forming a dimer (100 kDa) (Hendriks *et al.*, 2003). It has been proposed that the ferredoxin-thioredoxin system, which is influenced by light, has a major participation in the AGPase redox regulation (Schürmann and Buchanan, 2008). To monitor if TOR inhibition has an impact in changing AGPase redox state, immunoblotting technique was used to quantify its monomer or dimer forms (Kurien and Scofield, 2006).

As shown in the **Figure 4.11**, the amount of AGPase seemed to be different between AZD-8055 and DMSO-treated plants after 4h and 6h. In addition, the content of the inactive form (as dimer) tends to be higher in the control plants, indicating that the AGPase active form is more present in the AZD-8055 treated plants (**Figure 4.11A,B**).

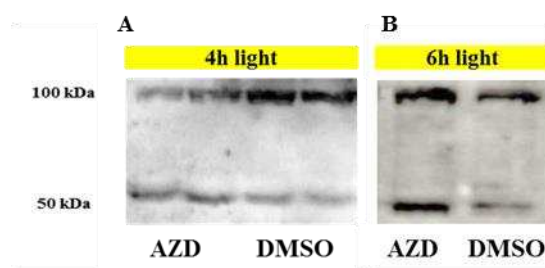


**Figure 4.11 - Immunoblotting of AGPase in AZD-treated plants and control plants.** Immunoblotting of AGPase of AZD or DMSO treated plants after (A) after 4 h or (B) 6h of the treatment in light (A). Upper band (100KDa) and lower band represent the dimeric and monomeric form, respectively. The results are the western from 26 plants/2 biological replicates; Yellow bar (light).

Taking together, these results indicated that TOR inhibition leads to changes in the redox status of the AGPase. However, these changes do not reflect in the changes of AGPase activity and consequently in the changes in the rate of starch synthesis.

#### 4.5 – Measurement of reduced and oxidized glutathione and the cellular redox status

Based on the results of the AGPase activity, one could speculate that TOR could regulate changes in the general redox status of the cell. Modifications in the redox state play important roles in modulating signaling linked to developmental processes and interactions with the environment (Queval and Noctor, 2007). Several biological processes and the major part of enzymes related to primary metabolism are subject to regulation mediated by the redox status of the cell (Tiessen *et al.*, 2002). In other eukaryotic species, it has already shown that the TOR signaling can control the redox state. To evaluate if TOR also modulates the cellular redox state in Arabidopsis, reduced (GSH) and oxidized (GSSG) forms of glutathione were measured in AZD- and DMSO-treated plants.

Glutathione is considered the major thiol-disulfide redox buffer of the cell (Noctor *et al.*, 2012). The redox state of a system is usually estimated by taking the ratio of  $[GSH]/[GSSG + GSH]$  or by using the Nernst equation ( $E = -240 - (59 \times 0.5) \log([GSH]^2/GSSG)$ ). This means that the reduction potential is dependent on the GSH/GSSG ratio and the absolute concentration of GSH.

As shown in **Figure 4.12 A, B**, total and reduced (GSH) glutathione forms were increased in TOR-inhibited plants after 12 hours of treatment, respectively. In contrast,



those levels tend to be similar in the AZD-8055 treated plants and control plants after 24h. The content of glutathione in its oxidized form was significantly different between treatments only at the time point 24 hours after treatment (**Figure 4.12 C**). It has been proved that oxidative stress results in the formation of GSSG at the expense of GSH. Low ratio of [GSH]/[GSSG] would change the redox state to a more positive potential and indicates oxidative stress (Schafer and Buettner, 2001). As shown in **Figure 4.12 D**, there was no significantly differences in [GSH]/[GSSG] ratio between treatments, indicating absence of oxidative stress after AZD-8055 treatment.

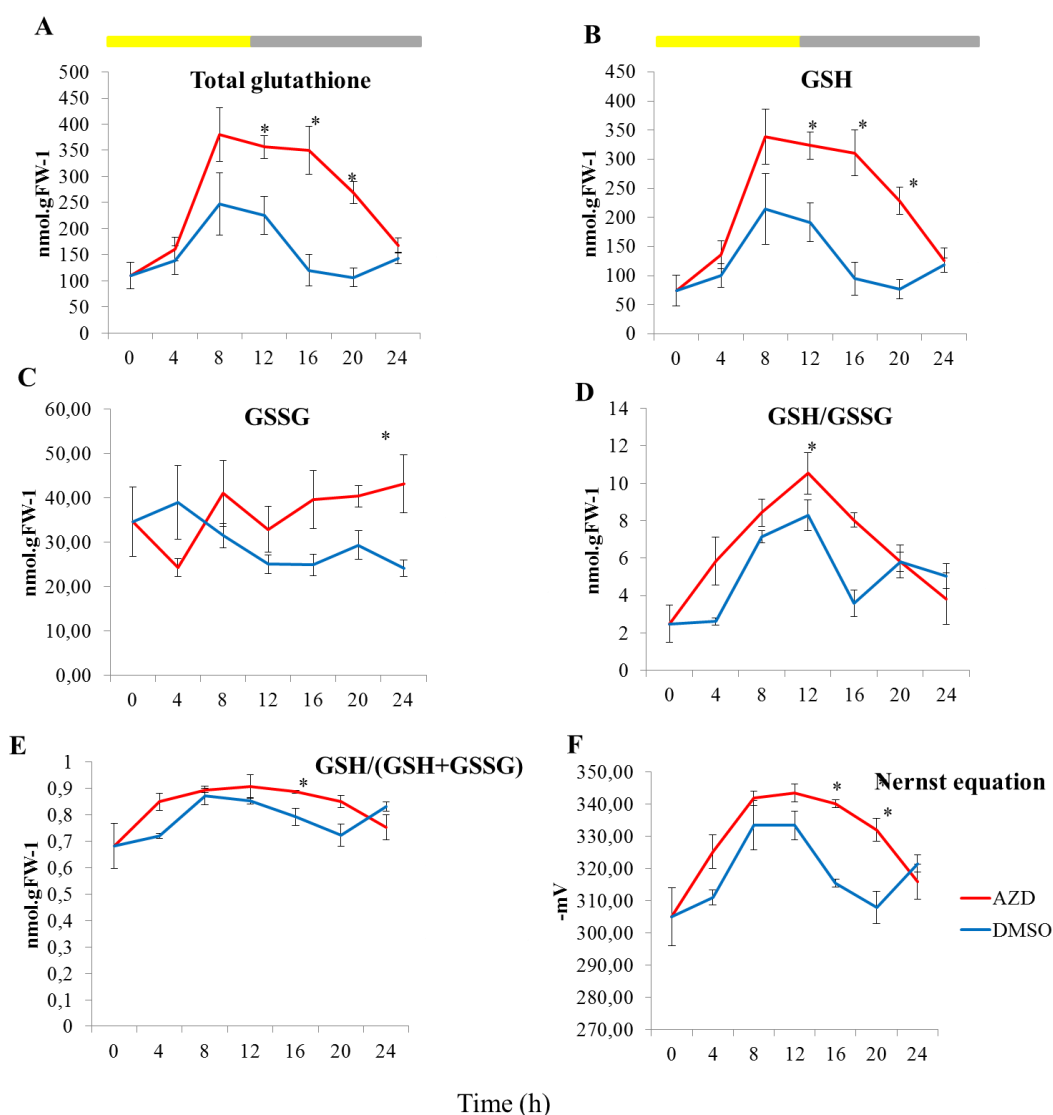


**Figure 4.12 – Measurement of glutathione and the redox status of the cell in AZD-treated plants and non-treated plants.**

(A) Total glutathione; (B) Reduced glutathione; (C) Oxidized glutathione; (D) GSH/GSSG ratio; (E) GSH/(GSH+GSSG) ratio; (F) Nernst equation. Samples of 11 days-old plants were harvested every 4h during the day (yellow bar) and every 4h during the night (grey bar) for 24h (26plants/4 replicates).



As shown in **Figure 4.12 E, F**, there were significantly statistical differences in the redox state between treatments for the time points 16h and 20h h after treatment by using [GSH]/[GSSG] ratio and Nernst equation, respectively. However, for every time point sampled, TOR-inhibited plants tended to have a redox potential more reduced compared to control. These results pointed to a possible influence of TOR in maintaining the reduced glutathione form in its homeostatic levels, since changes were observed for this metabolite after TOR-inhibition and consequently influencing the redox status of the cell. Due our kinetics analysis, it is likely that the redox state might not regulate the observed increase in starch synthesis after TOR inhibition. It remains to be elucidated, however, if those changes in the cellular redox status would regulate other enzymes involved in the primary metabolism as a secondary effect of TOR repression.

## 5 - Conclusions

In this work, a hydroponic system was established, allowing to investigate the short-term analysis of TOR repression by chemical inhibitors. This system opened new perspectives of investigating direct targets of the TOR signaling pathway in plants. As a proof of concept, this system was used to unravel the starch excess phenotype commonly found in transgenic lines targeting genes encoding for members of the TOR complex. Using a combination of diel cycle experiments and chemical inhibition of TORC, it was possible to verify that TOR inhibition leads to an increase in starch synthesis right after 4h of drug treatment. In agreement with the starch levels, levels of sucrose were decreased, whereas the levels of sugars involved in sucrose breakdown, such as fructose and glucose were increased. Furthermore, decreased in the levels of mannose and orthophosphate opened the perspective of investigating the role of TOR in the regulatory properties of AGPase, the first concomitant enzyme involved in starch synthesis. Although TOR inhibited plants displayed higher content of the active form of AGPase (monomer), enzymatic activity assays revealed that changes in AGPase activity might occur as secondary effect of TOR inhibition and might be not related to the starch excess phenotype observed 4 hours after AZD-treatment. Reduced and oxidized glutathione measurement showed that TOR may regulate the GSH content and impacts the redox status of the cell. Although these results might be important to investigate others aspects of the primary metabolism responses mediated by TOR, the cellular redox state seems not to be the main regulation for the observed starch excess phenotype.

The complex regulation of starch and C metabolism in plants opened the new perspectives to investigate other pathways where TOR might play a role as it is pointed in Figure 4.13. For example, enzymatic assays related to sucrose phosphate and other enzymes belonging to primary metabolism, a possible role played for TOR in respiration, among others.

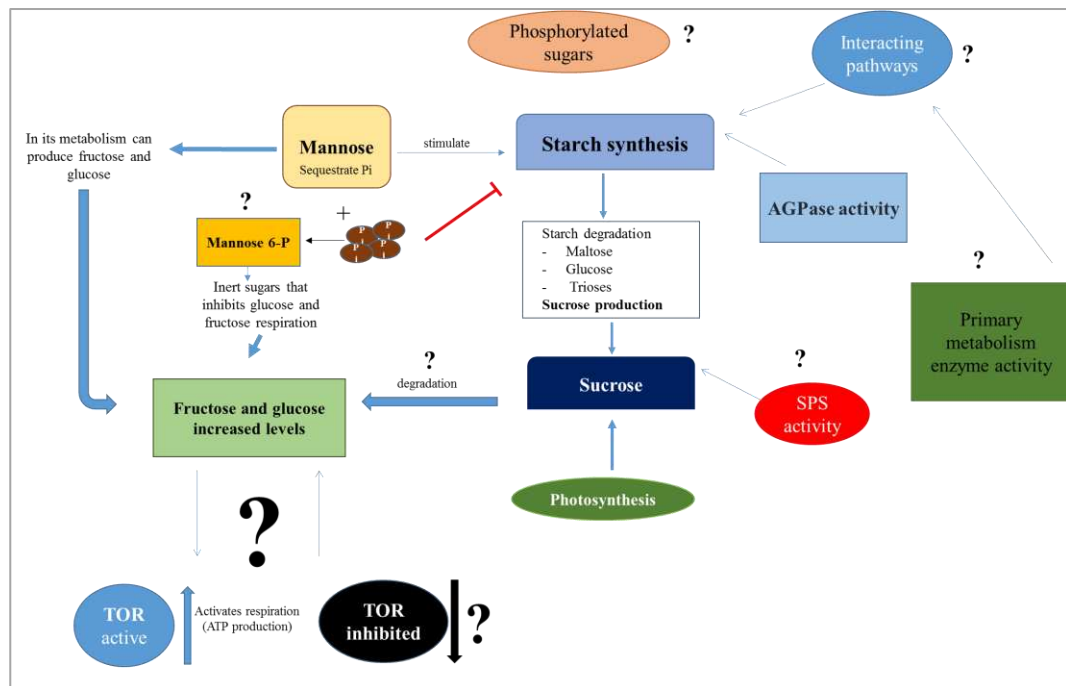


**Figure 5.1- Schematic representation for future investigations.**

The results obtained in this work raised several hypothesis on how TOR could modulate the starch synthesis.. Question marks represent new perspectives for studying the TOR regulation of starch and C metabolism.

## References

- Alarcon CM, Heitman J, Cardenas ME. **Protein kinase activity and identification of a toxic effector domain of the target of rapamycin TOR proteins in yeast.** *Mol Biol Cell*, 1999, 10:2531-46.
- Anderson GH, Veit B, Hanson MR. **The Arabidopsis *AtRaptor* genes are essential for post-embryonic plant growth.** *BMC Biology*, 2005, 12: 1741-7007.
- Andrade MA, Bork P. **HEAT repeats in the Huntington's disease protein.** *Nature genet.* 1995, 11:115-116.
- Ball S, Colleoni C, Cenci U, Raj JN, Tirtiaux C. **The evolution of glycogen and starch metabolism in eucaryotes gives molecular clues to understand the establishment of plastid endosymbiosis.** *Journal of Experimental Botany*, 2011, 62:1775-1801.
- Ball SG, Morell MK. **From bacterial glycogen to starch: understanding the biogenesis of the plant starch granule.** *Annu Rev Plant Biol.* 2003, 54:207-33.
- Baumberger N, Doesseger B, Guyot R, Diet A, Parsons RL, Clark MA, Simmons MP, Bedinger P, Goff SA, Ringli C, Keller B. **Whole-genome comparison of leucine-rich repeat extensins in Arabidopsis and rice: A conserved family of cell wall proteins form a vegetative and a reproductive clade.** *Plant Physiol.* 2003a, 131: 1313–1326.
- Baumberger N, Ringli C, and Keller B. **The chimeric leucine-rich repeat/extensin cell wall protein LRX1 is required for root hair morphogenesis in *Arabidopsis thaliana*.** 2001, *Genes Dev.* 15: 1128–1139.
- Baumberger N, Steiner M, Ryser U, Keller B, and Ringli C. **Synergistic interaction of the two paralogous *Arabidopsis* genes LRX1 and LRX2 in cell wall formation during root hair development.** *Plant J.* 2003b, 35: 71–81.
- Bentzinger CF, Romanino K, Cloetta D, Lin S, Mascarenhas JB, Oliveri F, Xia J, Casanova E, Costa CF, Brink M, Zorzato F, Hall MN, Ruegg MA. **Skeletal Muscle-Specific Ablation of raptor, but not of rictor, Causes Metabolic Changes and Results in Muscle Dystrophy.** *Cell Metab*, 2008, 8:411-24.
- Bosotti R, Isacchi A, Sonnhhammer EL. **FAT: a novel domain in PIK-related kinases.** *Trends Biochem Sci.* 2000, 25:225-7.
- Boyes DC, Zayed AM, Ascenzi R, McCaskill AJ, Hoffman NE, Davis KR, Görlach J. **Growth stage-based phenotypic analysis of *Arabidopsis* a model for high throughput functional genomics in plants.** *The Plant Cell*, 2001, 13:1499-1510.
- Caldana C, Li Y, Leisse A, Zhang Y, Bartholomaeus L, Fernie AR, Willmitzer L, Giavalisco P. **Systemic analysis of inducible Target of Rapamycin mutants reveal a general metabolic switch controlling growth in *Arabidopsis thaliana*.** *Plant J.* 2013, 73:897-909.
- Caldana C, Scheible WR, Mueller-Roeber B, Ruzicic S. **A quantitative RT-PCR platform for high-throughput expression profiling of 2500 rice transcription factors.** *Plant Methods.* 2007; 3: 7.
- Cao H, Imparl-Radosevich J, Guan H, Keeling PL, James MG, Myers AM. **Identification of the soluble starch synthase activities of maize endosperm.** *Plant Physiol.* 1999, 120:205-16.
- Caspar T, Huber SC, Somerville C. **Alterations in growth, photosynthesis, and respiration in a starchless mutant of *Arabidopsis thaliana* (L.) deficient in chloroplast phosphoglucomutase activity.** *Plant Physiol* 1985, 79:11-17.

- Castrillo JI, Zeef LA, Hoyle DC, Zhang N, Hayes A, Gardner DC, Cornell MJ, Petty J, Hakes L, Wardleworth L, Rash B, Brown M, Dunn WB, Broadhurst D, O'Donoghue K, Hester SS, Dunkley TP, Hart SR, Swainston N, Li P, Gaskell SJ, Paton NW, Lilley KS, Kell BD, Oliver SG. **Growth control of the eukaryote cell: a systems biology study in yeast.** *Journal of biology*, 2007, 6:4.
- Chauvin C, Koka V, Nouschi A, Mieulet V, Hoareau-Aveilla C, Dreazen A, Cagnard N, Carpentier W, Kiss T, Meyuhas O, et al. **Ribosomal protein S6 kinase activity controls the ribosome biogenesis transcriptional program.** 2013, *Oncogene* <http://dx.doi.org/>.
- Chresta CM, Davies BR, Hickson I, et al. **AZD8055 is a potent, selective, and orally bioavailable ATP-competitive mammalian target of rapamycin kinase inhibitor with in vitro and in vivo antitumor activity.** *Cancer Research*, 2010, 70: 288–298.
- Cornu M, Albert V, Hall MN. **mTOR in aging, metabolism, and cancer.** *Curr Opin Genet Dev.* 2013, 23:53-62
- Craig J, Lloyd JR, Tomlinson K, Barber L, Edwards A, Wang TL, Martin C, Hedley CL, Smith AM. **Mutations in the gene encoding starch synthase II profoundly alter amylopectin structure in pea embryos.** *Plant Cell*, 1998, 10:413-26.
- Cuadros-Inostroza A, Caldana C, Redestig H, Kusano M, Lisec J, Peña-Cortés H, Willmitzer L, Hannah MA. **TargetSearch - a Bioconductor package for the efficient preprocessing of GC-MS metabolite profiling data.** *BMC Bioinformatics*, 2009, 10:428.
- Czechowski T, Stitt M, Altmann T, Udvardi MK, Wolf-Rüdiger Scheible. **Genome-Wide Identification and Testing of Superior Reference Genes for Transcript Normalization in *Arabidopsis*.** *Plant Physiology*, 2005, 139:1 5-17.
- Dames SA, Mulet JM, Rathgeb-Szabo K, Hall MN, Grzesiek S. **The solution structure of the FATC domain of the protein kinase target of rapamycin suggests a role for redox-dependent structural and cellular stability.** *J Biol Chem.* 2005, 280:20558-64.
- Deprost D, Yao L, Sormani R, Moreau M, Leterreux G, Nicolai M, Bedu M, Robaglia C, Meyer C. **The Arabidopsis TOR kinase links plant growth, yield, stress resistance and mRNA translation.** *EMBO rep*, 2007, 8:864-870.
- Dobrenel T, Marchive C, Azzopardi M, Clément G, Moreau M, Sormani R, Robaglia C, Meyer C. **Sugar metabolism and the plant target of rapamycin kinase: a sweet operaTOR?** *Front Plant Sci.* 2013, 4: 93.
- Dowling RJ, Topisirovic I, Fonseca BD, Sonenberg N. **Dissecting the role of mTOR: lessons from mTOR inhibitors.** *Biochimica et Biophysica Acta*, 2010, 1804:433–439.
- Duvel K, Yecies JL, Menon S, Raman P, Lipovsky AL, Triantafellow E, Ma Q, Gorrski R, Cleaver S, Vander Heiden MG, MacKeigan JP, Finam PM, Clish CB, Murphy LO, Manning BD. **Activation of a metabolic gene regulatory network downstream of mTOR complex 1.** *Mol Cell*, 2010, 39:171-83.
- Edwards GE, Walker DA. **C3 C4: Mechanisms and cellular environmental regulation of photosynthesis.** Black-well. 1983.
- Figuerola CM, Fei R, Ishihara H, Watanabe M, Kolling K, Krause U, Hohne M, Encke B, Plaxton WC, Zeeman SC, Li Z, Schulze WX, Hoefgen R, Stitt Mohn, Lunn JE. **Trehalose 6-phosphate coordinates organic and amino acid metabolism with carbon availability.** *The Plant Journal* (2016) 85, 410–423.
- Flügge U., Fischer K, Gross A, Sebald W, Lottspeich F, Eckerskorn C. **The triose phosphate-3-phosphoglycerate-phosphate translocator from spinach chloroplasts:Nucleotide sequence**

- of a full-length cDNA clone and import of the *in vitro* synthesized precursor protein into chloroplasts.** *EMBOJ.* 1989 8:39-46.
- Franco R, Rosenfeld MG. **Hormonally inducible phosphorylation of a nuclear pool of ribosomal protein S6.** *J Biol Chem.* 1990, 265:4321-5.
- François JM, Walther T, Parrou JL. **Genetics and regulation of glycogen and trehalose metabolism in *Saccharomyces cerevisiae*.** *Springer*, 2012, 22:29-48.
- Gao M, Wanat J, Stinard PS, James MG, Myers AM. **Characterization of *dull1*, a maize gene coding for a novel starch synthase.** *Plant Cell*, 1998, 10:399-412.
- Garcia-Martinez JM, Moran J, Clarke RG, Gray A, Cosulich SC, Chresta CM, Alessi DR. **Ku-0063794 is a specific inhibitor of the mammalian target of rapamycin (mTOR).** *Biochemistry Journal*, 2009, 421:29-42.
- Geigenberger P, Kolbe A, Tiessen A. **Redox regulation of carbon storage and partitioning in response to light and sugars.** *J Exp Bot*, 2005, 416: 1469-79.
- Giavalisco P, Li Y, Matthes A, Eckhardt A, Hubberten HM, Hesse H, Segu S, Hummel J, Köhl K, Willmitzer L. **Elemental formula annotation of polar and lipophilic metabolites using (13) C, (15) N and (34) S isotope labelling, in combination with high-resolution mass spectrometry.** *Plant J.* 2011, 68:364-76.
- Gibon Y, Pyl ET, Sulpice R, Lunn JE, Höhne M, Günther M, Stitt M. **Adjustment of growth, starch turnover, protein content and central metabolism to a decrease of the carbon supply when *Arabidopsis* is grown in very short photoperiods.** *Plant, Cell and Environment* (2009) 32, 859-874.
- Gibon Y, Vigeolas H, Tiessen A, Geigenberger P, Stitt M. **Sensitive and high throughput metabolite assays for inorganic pyrophosphate, ADPGlc, nucleotide phosphates, and glycolytic intermediates based on a novel enzymic cycling system.** *Plant J.* 2002, 30:221-35.
- Gibon Y, Bläsing OE, Palacios N, Pankovic D, Hendriks JHM, Fisahn J, Höhne M, Günter M, Stitt M. **Adjustment of diurnal starch turnover to short days: Depletion of sugar during the night leads to a temporary inhibition of carbohydrate utilisation, accumulation of sugars and post-translational activation of ADPGlucose pyrophosphorylase in the following light period.** *The Plant Journal*, 2004, 39:847-862.
- Gibon Y, Usadel B, Bläsing OE, Kamlage B, Hoehne M, Trethewey R, Stitt M. **Integration of metabolite with transcript and enzyme activity profiling during diurnal cycles in *Arabidopsis* rosettes.** *Genome Biology*, 2006, 7: R76.
- Goldschmidt EE and Huber SC. **Regulation of Photosynthesis by End-Product Accumulation in Leaves of Plants Storing Starch, Sucrose, and Hexose Sugars.** *Plant Physiol.* 1992, 99:1443-1448.
- Graf A, Schlereth A, Stitt M, Smith AM. **Circadian control of carbohydrate availability for growth in *Arabidopsis* plants at night.** *PNAS*, 2010, 107: 9458-9463.
- Griffith OW. **Determination of glutathione and glutathione disulfide using glutathione reductase and 2-vinylpyridine.** *Anal Biochem.* 1980, 106:207-12.
- Hädrich N, Hendriks JH, Kötting O, Arrivault S, Feil R, Zeeman SC, Gibon Y, Schulze WX, Stitt M, Lunn JE. **Mutagenesis of cysteine 81 prevents dimerization of the APS1 subunit of ADP-glucose pyrophosphorylase and alters diurnal starch turnover in *Arabidopsis thaliana* leaves.** *Plant J.* 2012, 70:231-42.
- Hay N, Sonenberg N. **Upstream and downstream of mTOR.** *Genes Dev.* 2004, 18:1926-45.

- Harmer SL. **The circadian system in higher plants.** Annual Review of Plant Biology, 2009, 60: 357-377.
- Heldt HW, Chon CJ, Maronde D. **Role of orthophosphate and other factors in the regulation of starch formation in leaves and isolated chloroplasts.** *Plant Physiol.* 1977, 59:1146-55.
- Hendriks JHM, Kolbe A, Gibon Y, Stitt M, Geigenberger P. **ADP-Glucose Pyrophosphorylase Is Activated by Posttranslational Redox-Modification in Response to Light and to Sugars in Leaves of *Arabidopsis* and Other Plant Species.** *Plant Physiol.* 2003, 133: 838–849.
- Herold A, Lewis DH, Walker DA. Sequestration of cytoplasmic orthophosphate by mannose and its differential effect on photosynthetic starch synthesis in  $c_3$  and  $c_4$  species. *New phytologist*, 1976, 76:397-407.
- Hnilo J and Okita TW. **Mannose Feeding and Its Effect on Starch Synthesis in Developing Potato Tuber Discs.** WA, 1989, 99164-6340.
- Huber A, Bodenmiller B, Uotila A, Stahl M, Wanka S, Gerrits B, Aebersold R, Loewith R. **Characterization of the rapamycin-sensitive phosphoproteome reveals that Sch9 is a central coordinator of protein synthesis.** *Genes Dev.* 2009, 23: 1929–1943.
- Kavakli IH, Kato C, Choi SB, Kim KH, Salamone PR, Ito H, Okita TW. **Generation, characterization, and heterologous expression of wild-type and up-regulated forms of *Arabidopsis thaliana* leaf ADP-glucose pyrophosphorylase.** *Planta.* 2002, 215:430-439.
- King SP, Lunn JE, Furbank RT. **Carbohydrate Content and Enzyme Metabolism in Developing Canola Siliques.** *Plant Physiol.* 1997, 114:153-160.
- Klößgen RB, Gierl A, Schwarz-Sommer Z, Saedler H. **Molecular analysis of the waxy locus of *Zea mays*.** *Mol Gen Genet.* 1986, 203: 237–244.
- Kolbe A, Tiessen A, Schluepmann H, Paul M, Ulrich S, Geigenberger P. **Trehalose 6-phosphate regulates starch synthesis via posttranslational redox activation of ADP-glucose pyrophosphorylase.** *Proc Natl Acad Sci U S A.* 2005, 102:11118-23.
- Kötting O, Santelia D, Edner C, Eicke S, Marthaler T, Gentry MS, Comparot-Moss S, Chen J, Smith AM, Steup M, Ritte G, Zeeman SC. **STARCH-EXCESS4 Is a Laforin-Like Phosphoglucan Phosphatase Required for Starch Degradation in *Arabidopsis thaliana*.** *Plant cell*, 2009, 21:334-46.
- Kotting O, Kossman J, Zeeman SC, Lloyd JR. **Regulation of starch metabolism: the age of enlightenment.** *Curr Opin Plant Biol.* 2010, 13: 320–328.
- Krieg J, Hofsteenge J, Thomas G. **Identification of the 40 S ribosomal protein S6 phosphorylation sites induced by cycloheximide.** *J Biol Chem.* 1988, 263:11473-7.
- Kurien BT and Scofield RH. **Western blotting.** *Methods*, 2006, 38:283-93.
- Laplanche M, Sabatini DM. **mTOR signaling in growth control and disease.** *Cell*, 2012, 149:274-93.
- Leiber RM, John F, Verhertbruggen Y, Diet A, Knox JP, Ringli C. **The TOR pathway modulates the structure of cell walls in *Arabidopsis*.** *The plant cell*, 2010, 22: 1898–1908.
- Li J, Almagro G, Muñoz FJ, Baroja-Fernández E, Bahaji A, Montero M, et al. **Post-translational redox modification of ADP-glucose pyrophosphorylase in response to light is not a major determinant of fine regulation of transitory starch accumulation in *Arabidopsis* leaves.** *Plant Cell Physiol*, 2012:53:433–44.

- Li-Beisson Y, Shorrosh B, Beisson F, Andersson MX, Arondel V, Bates PD, Baud S, Bhatt K, Bird D, Debono A, Durrett TP, et al. Acyl-lipid metabolism. **The Arabidopsis Book/ American Society of Plant Biologists**. 2013, 11, e0161.
- Lin TP, Caspar T, Somerville C, Preiss J. **Isolation and characterization of a starchless mutant of *Arabidopsis thaliana* (L.) Heynh lacking ADPglucose pyrophosphorylase activity.** *Plant Physiol* 1988, 86:1131-1135.
- Lisec J, Schauer N, Kopka J, Willmitzer L, Fernie AR. **Gas chromatography mass spectrometry-based metabolite profiling in plants.** *Nat Protoc*. 2006, 1:387-96.
- Liu Q, Chang JW, Wang J, et al. **Discovery of 1-(4-(4-propionylpiperazin-1-yl)-3-(trifluoromethyl)phenyl)-9-(quinolin-3-yl)benzo[h][1,6]naphthyridin-2(1H)-one as a highly potent, selective mammalian target of rapamycin (mTOR) inhibitor for the treatment of cancer.** *Journal of Medicinal Chemistry*, 2010, 53:7146–7155.
- Liu Q, Wang J, Kang SA, Thoreen CC, Hur W, Ahmed T, Sabatini DM, Gray NS. **Discovery of 9-(6-aminopyridin-3-yl)-1-(3-(trifluoromethyl)phenyl)benzo[h][1,6]naphthyridin-2(1H)-one (Torin2) as a potent, selective, and orally available mammalian target of rapamycin (mTOR) inhibitor for treatment of cancer.** *Journal of Medicinal Chemistry*, 2011, 54:1473–1480.
- Liu Y, Bassham DC. **TOR is a negative regulator of autophagy in *Arabidopsis thaliana*.** *Plos One*, 2010, 5(7):e11883.
- Lu Y1, Gehan JP, Sharkey. **Daylength and circadian effects on starch degradation and maltose metabolism.** *TD. Plant Physiol*. 2005, 138:2280-91.
- Lunn JE, Feil R, Hendriks JH, Gibon Y, Morcuende R, Osuna D, Scheible WR, Carillo P, Hajirezaei MR, Stitt M. **Sugar-induced increases in trehalose 6-phosphate are correlated with redox activation of ADPglucose pyrophosphorylase and higher rates of starch synthesis in *Arabidopsis thaliana*.** *Biochem J*. 2006, 397:139-48.
- Martin DE, Souillard A, Hall MN. **TOR regulates ribosomal protein gene expression via PKA and the Forkhead transcription factor FHL1.** *Cell*, 2004, 119: 969–979.
- Martins MCM, Hejazi M, Fettke J, Steup M, Feil R, Krause U, Arrivault S, Vosloh D, Figueroa CM, Ivakov A, YadavUP, Piques M, Metzner D, StittM, Lunn JE. **Feedback Inhibition of Starch Degradation in *Arabidopsis* Leaves Mediated by Trehalose 6-Phosphate.** *Plant Physiol*. 2013, 163:1142-63.
- Matt P, Geiger M, Walch-Liu P, Engels C, Krapp A, Stitt M. **Elevated carbon dioxide increases nitrate uptake and nitrate reductase activity when tobacco is growing on nitrate, but increases ammonium uptake and inhibits nitrate reductase activity when tobacco is growing on ammonium nitrate.** *Plant, Cell & Environment*, 2001, 24:1119–1137.
- Menand B, Desnos T, Nussaume L, Berger F, Bouchez D, Meyer C, Robaglia C. **Expression and disruption of the *Arabidopsis* TOR (target of rapamycin) gene.** *Proc Nall Acad Sci U.S.A*, 2002, 99: 6422-7.
- Montané MH, Menand B. **ATP-competitive mTOR kinase inhibitors delay plant growth by triggering early differentiation of meristematic cells but no developmental patterning change.** *Journal of Experimental Botany*, 2013, 64:4361–4374.
- Moreau M, Azzopardi M, Clément G, Dobrenel T, Marchive C, Renne C, Martin-Magniette ML, Taconnat L, Renou JP, Robaglia C, Meyer C. **Mutations in the *Arabidopsis* homolog of LST8/GβL, a partner of the target of Rapamycin kinase, impair plant growth, flowering, and metabolic adaptation to long days.** *Plant Cell*, 2012, 2:463-81.



- Morell MK, Bloom M, Knowles V, Preiss J. **Subunit Structure of Spinach Leaf ADPglucose Pyrophosphorylase.** *Plant Physiol*, 1987, 85:182-187.
- Mugford ST, Fernandez O, Brinton J, Fils A, Krohn N, Encke B, Feil R, Sulpice R, Lunn JE, Stitt M, Smith AM. **Regulatory properties of ADP glucose pyrophosphorylase are required for adjustment of leaf starch synthesis in different photoperiods.** *Plant physiol.* 2014, 166:1733-47.
- Neuhaus HE, Stitt M. **Control analysis of photosynthate partitioning. Impact of reduced activity of ADP-glucose pyrophosphorylase or plastid phosphoglucomutase on the fluxes to starch and sucrose in *Arabidopsis thaliana* (L.)** *Henyh. Planta*, 1990, 182:445-454
- Noctor G, Mhamdi A, Chaouch S, Han Y, Neukermans J, Marquez-Garcia B, Queval G, Foyer CH. **Glutathione in plants: an integrated overview.** *Plant, Cell and Environment*, 2012, 35: 454–484.
- Nunes C, O'Hara LE, Primavesi LF, Delatte TL, Schluepmann H, Somsen GW, Silva AB, Fevereiro PS, Winger A, Paul MJ. **The Trehalose 6-Phosphate/SnRK1 Signaling Pathway Primes Growth Recovery following Relief of Sink Limitation.** *Plant Physiology*, 2013, 162:1720-1732.
- Okita TW, Nakata PA, Anderson JM, Sowokinos J, Morell M, Preiss J. **The Subunit Structure of Potato Tuber ADPglucose Pyrophosphorylase.** *Plant Physiol*, 1990, 93:785-90.
- Pantin F, Simonneau T, Rolland G, Dauzat M, Muller B. **Control of Leaf Expansion: A Developmental Switch from Metabolics to Hydraulics.** *Plant physiology*, 2011, 156:803–815.
- Pérez-Pérez ME, Florencio FJ, Creso JL. **Inhibition of target of rapamycin signaling and stress activate autophagy in *Chlamydomonas reinhardtii*.** *Plant physiol.* 2010, 152:1874-88.
- Perry J, Kleckner N. **The ATRs, ATMs, and TORs are Giant HEAT repeat proteins.** *Cell*, 2003, 112:151-155.
- Queval G, Noctor G. **A plate reader method for the measurement of NAD, NADP, glutathione, and ascorbate in tissue extracts: Application to redox profiling during *Arabidopsis* rosette development.** *Anal Biochem.* 2007, 363:58-69
- Ren M, Qiu S, Venglat P, Xiang D, Feng L, Selvaraj G, Datla R. **Target of rapamycin regulates development and ribosomal RNA expression through kinase domain in *Arabidopsis*.** *Plant Physiol.* 2011, 155:1367–1382.
- Ren M, Venglat P, Qiu S, Feng L, Cao Y, Wang E, Xiang D, Wang J, Alexander D, Chalivendra S, Logan D, Matto A, Selvaraj G, Datla R. **Target of rapamycin signaling regulates metabolism, growth, and life span in *Arabidopsis*.** *Plant cell*, 2012, 24:4850-74.
- Robaglia C, Thomas M, Meyer C. **Sensing nutrient and energy status by SnRK1 and TOR kinases.** *Curr Opin Plant Biol.* 2012, 15:301-7.
- Ruan YL. **Sucrose Metabolism: Gateway to Diverse Carbon Use and Sugar Signaling.** *Annu. Rev. Plant Biol.* 2014, 65:33–67.
- Ruvinsky I, Meyuhas O. **Ribosomal protein S6 phosphorylation: from protein synthesis to cell size.** *Trends Biochem Sci*, 2006, 31:342-8.
- Santelia D, Zeeman SC. **Progress in *Arabidopsis* starch research and potential biotechnological applications.** *Curr Opin Biotechnol.* 2011, 22:271-80.
- Schafer FQ, Buettner GR. **Redox environment of the cell as viewed through the redox state of the glutathione disulfide/glutathione couple** *Free Radical Biology and Medicine*, 2001, 30: 1191–1212.

- Schluepmann H, Pellny T, van Dijken A, Smeekens S, Paul M. **Trehalose 6-phosphate is indispensable for carbohydrate utilization and growth in *Arabidopsis thaliana*.** *Proc Natl Acad Sci USA*, 2003, 100: 6849–6854.
- Schmelzle T, Beck T, Martin DE, Hall MN. **Activation of the RAS/Cyclic AMP Pathway Suppresses a TOR Deficiency in Yeast.** *Mol Cell Biol*. 2004, 24:338-51.
- Schurmann P and Buchanan BB. **The Ferredoxin/Thioredoxin System of Oxygenic Photosynthesis.** *Antioxidants & redox signaling*. 2008, 10: 1235-1274.
- Scott P, Lange AJ, Pilkis S, Kruger NJ. **Carbon metabolism in leaves of transgenic tobacco (*Nicotiana tabacum* L.) containing elevated fructose 2,6-bisphosphate levels.** *Plant J*, 1995, 7: 461-469.
- Shure M, Wessler S, Fedoroff N. **Molecular identification and isolation of the Waxy locus in maize.** *Cell*. 1983, 35:225-33.
- Smith AM, Stitt M. **Coordination of carbon supply and plant growth.** *Plant Cell Environ*. 2007, 30:1126-49.
- Sokolov LN, Dominguez-Solis JR, Allary AL, Buchanan BB, Luan S. **A redox-regulated chloroplast protein phosphatase binds to starch diurnally and functions in its accumulation.** *Proc Natl Acad Sci U S A*. 2006, 103: 9732–9737.
- Sonnenwald U, Kossmann J. **Starches-from current models to genetic engineering.** *Plant Biotechnol J*. 2013, 2:223-32.
- Stitt M, Lilley RM, Gerhardt R, Heldt HW. **Metabolite levels in specific cells and subcellular compartments of plant leaves.** *Methods Enzymol*. 1989, 174:518–552.
- Stitt M, Zeeman SC. **Starch turnover: pathways, regulation and role in growth.** *Curr Opin Plant Biol*. 2012, 15:282-92.
- Sulpice R, Fills A, Ivakov AA, Apelt F, Krohn N, Encke B, Abel C, Feil R, Lunn JE, Stitt M. ***Arabidopsis* coordinates the diurnal regulation of carbon allocation and growth across a wide range of photoperiods.** *Molecular Plant*, 2014, 7: 137-155.
- Sulpice R, Pyl ET, Ishihara H, Trenkamp S, Steinfath M, Witucka-Wall H, Gibon Y, Usadela B, Poreea F, Piques MC, Korff MV, Steinhauser MC, Keurentjes JJB, Guenthera M, Hoehne M, Selbig J, Fernie AR, Altmann T, Stitt M. **Starch as a major integrator in the regulation of plant growth.** *Proc Natl Acad Sci U S A*. 2009, 106:10348-53.
- Taiz L, Zeiger E. *Plant Physiology*, Fifth Edition. Sinauer Associates. Sunderland, 2010, MA. (In press).
- Tatematsu K, Ward S, Leyser O, Kamiya Y, Nambara E. **Identification of cis-Elements That Regulate Gene Expression during Initiation of Axillary Bud Outgrowth in *Arabidopsis*.** *Plant Physiology*, 2005,138:757–766.
- Thoreen CC, Kang SA, Chang JW, Liu Q, Zhang J, Gao Y, Reichling LJ, Sim T, Sabatini DM, Gray NS. **An ATPcompetitive mammalian target of rapamycin inhibitor reveals rapamycin-resistant functions of mTORC1.** *Journal of Biological Chemistry*, 2009 284:8023–8032.
- Tiessen A, Hendriks JH, Stitt M, Branscheid A, Gibon Y, Farré EM, Geigenberger P. **Starch synthesis in potato tubers is regulated by post-translational redox modification of ADP-glucose pyrophosphorylase: a novel regulatory mechanism linking starch synthesis to the sucrose supply.** *Plant Cell*, 2002, 14:2191-213.
- Tsang CK, Qi H, Leroy F. L, Zheng XFS. **Targeting mammalian target of rapamycin (mTOR) for health and diseases.** *Drug discovery today*, 2007, 12:112–124.

- Weckwerth W, Wenzel K, Fiehn O. **Process for the integrated extraction, identification and quantification of metabolites, proteins and RNA to reveal their co-regulation in biochemical networks.** *Proteomics*, 2004, 4:78-83.
- Weise SE, Aung K, Jarou ZJ, Mehrshahi P, Li Z, Hardy AC, Carr DJ, Sharkey TD. **Engineering starch accumulation by manipulation of phosphate metabolism of starch.** *Plant Biotech J*, 2012, 7:139- 141.
- Wingler A, Delatte TL, O'Hara LE, Primavesi LF, Jhurreea D, Paul MJ, Schluepmann H. **Trehalose 6-Phosphate Is Required for the Onset of Leaf Senescence Associated with High Carbon Availability.** *Plant Physiology*, 2012, 158:1241-125.
- Wullschleger S, Loewith R, Hall MN. **TOR signaling in growth and metabolism.** *Cell*, 2006, 124:471–484.
- Wullschleger S, Loewith R, Oppliger W, Hall MN. **Molecular organization of target of rapamycin complex2.** *J Biol Chem*. 2005, 280:30697-704.
- Xiong Y, McCormack M, Li L, Hall Q, Xiang C, Sheen J. **Glucose-TOR signalling reprograms the transcriptome and activates meristems.** *Nature*, 2013, 496: 181–186.
- Xiong Y, Sheen J. Rapamycin and glucose-target of rapamycin (TOR) protein signalling in plants. *J Biol Chem*, 2012, 287:2836-42.
- Xiong Y, Sheen J. **The role of the Target of Rapamycin signalling networks in Plant growth and Metabolism.** *Plant physiology*, 2014, 164:499-512.
- Yadav UP, Ivakov A, Feil R, Duan GY, Walther D, Giavalisco P, Piques M, Carillo P, Hubberten HM, Stitt M, Lunn JE. **The sucrose-trehalose 6-phosphate (Tre6P) nexus: specificity and mechanisms of sucrose signalling by Tre6P.** *J Exp Bot*. 2014, 65:1051-68.
- Yu K, Shi C, Toral-Barza L. **Beyond rapalog therapy: preclinical pharmacology and antitumor activity of WYE-125132, an ATP-competitive and specific inhibitor of mTORC1 and mTORC2.** *Cancer Research*, 2010, 70:621–631.
- Yu K, Toral-Barza L, Shi C, Zhang WG, Lucas J, Shor B, Kim J, Verheijen J, Curran K, Malwitz DJ et al. **Biochemical, cellular, and in vivo activity of novel ATP-competitive and selective inhibitors of the mammalian target of rapamycin.** *Cancer Research*, 2009, 69:6232–6240.
- Zeeman SC, Kossmann J, Smith AM. **Starch: its metabolism, evolution, and biotechnological modification in plants.** *Annu Rev Plant Biol*. 2010, 61: 209–234.
- Zeeman SC, Smith SM, Smith AM. **The diurnal metabolism of leaf starch.** *Biochem J*. 1, 401:13-28.
- Zhang X, Colleoni C, Ratushna V, Sirghie-Colleoni M, James MG, Myers AM. **Molecular characterization demonstrates that the Zea mays gene sugary2 codes for the starch synthase isoform SSIIa.** *Plant Mol Biol*. 2004, 54:865-79.
- Zhang Y, Primavesi LF, Jhurreea D, Andralojc PJ, Mitchell RA, Powers SJ, Schluepmann H, Delatte T, Wingler A, Paul M.J. **Inhibition of SNF1-related protein kinase1 activity and regulation of metabolic pathways by trehalose-6-phosphate.** *Plant Physiol*. 2009, 149: 1860–1871.
- Zhang YJ, Duan Y, Zheng XF. **Targeting the mTOR kinase domain: the second generation of mTOR inhibitors.** *Drug Discovery Today*, 2011, 16:325–331.

## Supplemental data

**Table 1:** Primers used in this work.

Gene name	Forward primer sequence 5' to 3'	Forward primer sequence 5' to 3'
<i>APL1</i>	GTTCCCATTTGGAATAGGAGAGAACAC	GACCTATCTGCTTCTTGTATTCCCTC
<i>APL2</i>	TGGTCATAGCGAATGCAGATGGCGTG	AATGGTGGCGTTCTTCAGCACAACGG
<i>APL3</i>	CGGATTGTAAATTCGGTAATCTCAC	GCTCCTAACATAAGAGTATCCTGAAG
<i>APL4</i>	GCTAATTTAGCTCTTGTTGAGGAGCG	GGAGGAACCGAGGAGAAGTGTAGAAC
<i>L35a</i>	TTCTGAAGGCAACTGCTAATTTCTT	TGGCGTCCTTTCACCATTTT
<i>EFTu</i>	CCTGTTTCGCGTCCTTGACA	ACGTCCTTGAATTGAGAAAACATCT
<i>L14</i>	TCTCTTCGCCGCACAATTG	TCCACGAATCTCTTAAAACCCATT
<i>ARP</i>	GGTTGCCGCTGCTTTCC	CAGCAGAAGGATTAGCGTTTCC
<i>L19</i>	AATGAAATGCGGGAAAGGAAA	CCTGGAATTGGCCATAGAGATATC
<i>CPN10A</i>	ATGGGCATCAATCACATGGA	AGATTACGGAAAAGCACAAAATGAG
<i>TOR1</i>	AAGTCCCCCAATTAGCACTGCT	TTCGTCAGGCTCAACATCAGC

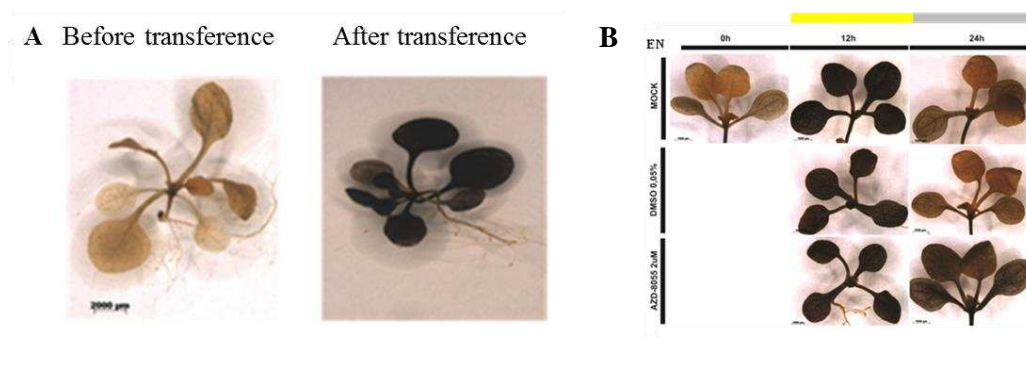


**Figure S1:** Lugol iodine-staining of seedlings treated with AZD – 8055 and DMSO (control) sampled every 12h for 24h.

(A) Iodine staining before and after medium transference; (B) Iodine staining of AZD-treated and non-treated plants. AZD-8055 2 µM and DMSO 0,05% were applied at the end of night. Samples were stained with lugol iodine to verify qualitatively the content of starch between treatments.